



# A Comparative Review of Electrolytes for Organic-Material-Based Energy-Storage Devices Employing Solid Electrodes and Redox Fluids

Ruiyong Chen,<sup>\*,[a]</sup> Dominic Bresser,<sup>\*,[b, c]</sup> Mohit Saraf,<sup>[b, c]</sup> Patrick Gerlach,<sup>[d]</sup> Andrea Balducci,<sup>\*,[d]</sup> Simon Kunz,<sup>[e, f]</sup> Daniel Schröder,<sup>\*,[e, f]</sup> Stefano Passerini,<sup>[b, c]</sup> and Jun Chen<sup>[g]</sup>

Electrolyte chemistry is critical for any energy-storage device. Low-cost and sustainable rechargeable batteries based on organic redox-active materials are of great interest to tackle resource and performance limitations of current batteries with metal-based active materials. Organic active materials can be used not only as solid electrodes in the classic lithium-ion battery (LIB) setup, but also as redox fluids in redox-flow batteries (RFBs). Accordingly, they have suitability for mobile and sta-

tionary applications, respectively. Herein, different types of electrolytes, recent advances for designing better performing electrolytes, and remaining scientific challenges are discussed and summarized. Due to different configurations and requirements between LIBs and RFBs, the similarities and differences for choosing suitable electrolytes are discussed. Both general and specific strategies for promoting the utilization of organic active materials are covered.

[a] Dr. R. Chen

Transfercenter Sustainable Electrochemistry  
Saarland University, 66123 Saarbrücken (Germany)  
E-mail: ruiyong.chen@uni-saarland.de  
hc18chen@gmail.com

[b] Dr. D. Bresser, Dr. M. Saraf, Prof. Dr. S. Passerini  
Helmholtz Institute Ulm (HIU)  
89081 Ulm (Germany)


[c] Dr. D. Bresser, Dr. M. Saraf, Prof. Dr. S. Passerini  
Karlsruhe Institute of Technology (KIT)  
76021 Karlsruhe (Germany)  
E-mail: dominic.bresser@kit.edu


[d] P. Gerlach, Prof. Dr. A. Balducci  
Institute for Technical Chemistry and Environmental Chemistry  
Center for Energy and Environmental Chemistry Jena (CEEC Jena)  
Friedrich-Schiller-Universität Jena  
07743 Jena (Germany)  
E-mail: andrea.balducci@uni-jena.de


[e] S. Kunz, Dr. D. Schröder  
Institute of Physical Chemistry  
Justus Liebig University Giessen  
35392 Gießen (Germany)  
E-mail: daniel.schroeder@phys.chemie.uni-giessen.de

[f] S. Kunz, Dr. D. Schröder  
Center for Materials Research (LaMa)  
Justus Liebig University Giessen  
35392 Gießen (Germany)

[g] Prof. Dr. J. Chen  
Key Laboratory of Advanced Energy Materials Chemistry  
Renewable Energy Conversion and Storage Center  
College of Chemistry, Nankai University  
Tianjin 300071 (P. R. China)

 The ORCID identification number(s) for the author(s) of this article can be found under:  
<https://doi.org/10.1002/cssc.201903382>.

 © 2020 The Authors. Published by Wiley-VCH Verlag GmbH & Co. KGaA. This is an open access article under the terms of Creative Commons Attribution NonCommercial License, which permits use, distribution and reproduction in any medium, provided the original work is properly cited and is not used for commercial purposes.

 This publication is part of a Special Issue focusing on "Organic Batteries". Please visit the issue at <http://doi.org/10.1002/cssc.v13.9>.

## 1. Introduction

With the booming development of electrochemical energy-storage systems from transportation to large-scale stationary applications, future market penetration requires safe, cost-effective, and high-performance rechargeable batteries.<sup>[1]</sup> Limited by the abundance of elements, uneven resource distribution and difficulties for recycling, it is considered that metal-based batteries would be too expensive for scale-up to large-scale systems.<sup>[2]</sup> In addition, state-of-the-art battery technologies, such as lithium-ion batteries (LIBs) and vanadium redox-flow batteries (RFBs), as representatives for portable and stationary batteries, respectively, are approaching their performance limitations, in terms of maximum capacity for reversibly hosting lithium cations<sup>[3–5]</sup> and the solubility of vanadium species.<sup>[6]</sup> In comparison, the search for alternatives to realize sustainable battery chemistries by using organic redox-active materials is very promising.<sup>[7–10]</sup> Organic materials can be obtained through synthetic chemistry or from renewable and sustainable resources. Their structural variability allows the tuning of the redox potential, stability, and theoretical capacity by carefully designing the versatile molecular structure and functional groups. With good flexibility, organic materials are also suitable as electrodes in flexible electronics.<sup>[11–13]</sup>

Interestingly, organic redox materials have shown broad applicability in LIBs,<sup>[7]</sup> beyond-Li systems (such as Na<sup>+</sup>, K<sup>+</sup>, and multivalent cations including Mg<sup>2+</sup>, Ca<sup>2+</sup>, Zn<sup>2+</sup>, or Al<sup>3+</sup>),<sup>[14–18]</sup> and RFBs.<sup>[19–22]</sup> The first two use organic materials as solid electrodes assembled inside the electrochemical cell (Figure 1), whereas RFBs store energy by using the electrochemical reactions of organic materials as dissolved species that are transported to reaction sites in the battery by the forced flow of redox electrolytes. Thus, RFBs utilize external tanks to store the liquid redox electrolytes and pumps to circulate the electrolytes.<sup>[23]</sup> The electrode materials for RFBs are typically porous

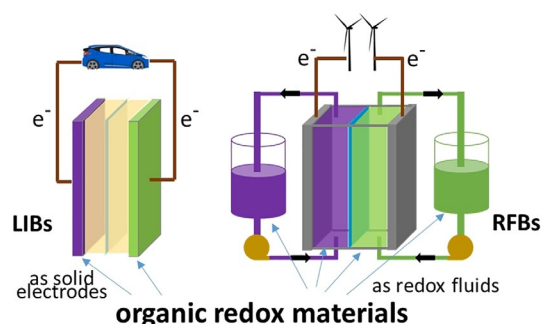


**Figure 1.** Schematic illustration of the use of sustainable organic energy-storage materials in LIBs and beyond-lithium batteries as solid electrodes, and in RFBs as redox fluids, the different system architectures and components of LIBs and RFBs for transportation and stationary applications, respectively.

carbon-based materials in thick felt (ca. mm) or thin paper (ca.  $\mu\text{m}$ ) forms, perfused by the liquid redox electrolytes.<sup>[24]</sup> The general architecture of RFBs offers the advantage of decoupling energy storage and power output capability by individually changing the volume of the redox electrolytes (i.e., the tank size) and the electrode area (i.e., the cell size), respectively.<sup>[23]</sup>

As compared in Figure 1, LIBs and beyond-lithium batteries use porous polymer separators to allow the transport of ionic

species between the cathode and anode, and to isolate the two electrodes electronically. The same electrolyte is commonly used in the two compartments of the electrochemical cell. The organic redox electrode materials should be ideally insoluble in the electrolyte media. In contrast, for RFBs, the redox fluids, that is, the anolyte and catholyte, contain active materials of different types and/or oxidation states, which are separated by either an ion-exchange membrane or a porous size-exclusion membrane.<sup>[25]</sup> Cross-contamination of the anolyte and catholyte due to the diffusion of fluidic redox species through the membranes in RFBs is often inevitable and should be minimized. The transport rate of charge-balancing ions through the membranes and the chemical diffusion of active species in the bulk electrolytes largely affect the power performance of RFBs. In addition, for RFBs, the organic materials need high solubility in the supporting electrolytes to achieve a high volumetric capacity.<sup>[26,27]</sup>

For organic, solid electrode materials, reversible charge storage occurs through an ion-coordination mechanism and/or the adsorption/desorption of electrolyte ions.<sup>[8,16,28–30]</sup> Accordingly, the electrochemical behavior of organic electrodes depends less on the type and radius of the charge-carrier ions. This is different from inorganic intercalation materials for which the reaction rates could be limited by the (de)solvation process at the electrode/electrolyte interface. However, some challenges remain to be solved, such as the unwanted high solubility of

Ruiyong Chen received his Ph.D. (summa cum laude) in 2011 from Saarland University, Germany, with a study on electrocatalysts for electrolytic chlorine production. Later, he did his postdoctoral research on intercalation materials for lithium-ion batteries at the Karlsruhe Institute of Technology, Germany. In 2015, he joined KIST Europe in Saarbrücken, leading efforts for developing novel electrolytes for redox flow batteries. In September 2016, he started his Habilitation at Saarland University.



Andrea Balducci is Professor for Applied Electrochemistry at the Institute for Technical Chemistry and Environmental Chemistry and at the Center for Energy and Environmental Chemistry Jena (CEEC Jena) of the Friedrich-Schiller University Jena, Germany. He is working on the development and characterization of novel electrolytes and active/inactive materials suitable for the realization of safe and high-performance supercapacitors, metal-ion batteries, and polymeric batteries.



Dominic Bresser is serving as group leader at the Helmholtz Institute Ulm (HIU), which is affiliated with the Karlsruhe Institute of Technology (KIT), Germany, focusing especially on the development of alternative anode materials, polymer electrolytes, and aqueous cathode processing technologies for lithium batteries. Prior to this, he held a postdoctoral position and Eurotalents Fellowship at CEA in Grenoble, France, after he completed his Ph.D. at Münster University, Germany.



Daniel Schröder received his Ph.D. with distinction in process engineering from TU Braunschweig in 2015, researching secondary zinc–oxygen batteries. Afterwards, he joined the Institute of Physical Chemistry at Justus-Liebig University Giessen as a junior group leader. His research group focuses on the fundamental understanding and improvement of redox-flow batteries, as well as Li-, Na-, and Zn-based metal–oxygen batteries by using model-based and operando techniques.



organic electrode materials in aprotic electrolytes, detrimental reactions at the electrode/electrolyte interface, ion trapping, and rapid self-discharge.<sup>[14]</sup>

For both LIBs and RFBs, new strategies towards the rational design of superior electrolyte formulations, allowing for an optimized battery performance, are very important to speed up the utilization of organic materials. The selection of suitable electrolytes should consider the safety of the solvent, the dissolution and chemical stability of the charge-carrier ions, the associated transport within the electrolyte, the ionic conductivity and electrochemical stability of both solvent and ions, the operating temperature range, and so forth.<sup>[31]</sup> The electrolyte compositions, which are widely investigated for inorganic electrode materials, are empirically selected as a starting point on the way to the further development of organic electrode materials. They include organic solvents that can assure a high operating voltage; ionic liquids (ILs) that are potentially non-flammable and often characterized by high electrochemical stability; polymers towards all-solid-state batteries, while allowing the use of size-exclusion membranes in RFBs; as well as aqueous systems that are cheap, safe, and may have high power densities due to the high ionic conductivity. Meanwhile, drawbacks for choosing these electrolytes also need to be considered, such as the generally limited operating voltage (<1.5 V) of water-based electrolytes,<sup>[32]</sup> high flammability and often toxicity of organic solvents, and high viscosity and poor transport properties of ILs.<sup>[33,34]</sup> The same applies for the RFB electrolytes.<sup>[24,26,27,35]</sup> Depending on the polarity, functional groups, and costs for the synthesis of organic active materials, different solvents and conducting ions with good chemical compatibility need to be selected.

Herein, based on the different working principles and characteristics of organic redox solid electrodes and organic redox fluids, we focus on the discussion and comparison of the electrolyte formulation, particularly with respect to important parameters, such as safety,<sup>[31]</sup> output voltage, cycling stability, and rate performance, in two distinct classes of rechargeable batteries: LIBs and RFBs. We provide an overview of the current status and perspectives for future optimization. Typical electrolyte components, including different solvents (organic solvents and water), ionic salts, and polymers, and the related challenges and opportunities for designing high-performance batteries are discussed.

## 2. Electrolytes for Redox Organic Electrodes

The requirements for an ideal electrolyte for organic electrode materials are, to a certain extent, the same as those for inorganic materials. It must have a high ionic conductivity for sufficiently fast (dis)charge of the cell, be (electro)chemically inert towards all other cell components, provide high safety, low toxicity, low cost, and be accompanied by a wide electrochemical stability window (ESW).<sup>[31,36–38]</sup> There are, however, some differences. First, an ESW of about 3.5 to 4.0 V is commonly sufficient, since most positive electrode materials are electrochemically active at about 3.0 V.<sup>[39–41]</sup> Second, the charge-carrier diffusion in the active-material particles is sometimes limited

and requires electrolytes that can easily access highly porous electrode architectures, especially if the focus is on high-power applications. Third, in the case of organic radical battery materials, the conducting salt is actively involved in the (dis)charge process. The cost penalty should be considered if a high concentration of salt is applied. With this in mind, we discuss different electrolyte systems, from conventional organic-solvent-based electrolytes to ionic-liquid- and polymer-based electrolytes, and finally, the latest progress in highly concentrated and environmentally friendly water-based electrolyte systems is highlighted.

### 2.1. Conventional organic-solvent-based electrolytes

Liquid organic-solvent-based electrolytes are the most investigated electrolyte systems used in combination with organic active battery materials.<sup>[42]</sup> These electrolytes consist of a conductive salt dissolved in a liquid organic solvent. To provide practical ion transport and sufficient charge compensation during the charge/discharge process, the salts and solvents utilized have to meet specific requirements. In general, the salt used should provide high ion mobility, and thus, high ionic conductivity, chemical inertness towards all cell components, and oxidative and reductive stability. In addition, it should completely dissociate in the solvent. Meanwhile, the solvent should have a high dielectric constant to dissolve the salt in a reasonable amount, a low viscosity, a broad ESW, and a wide operating temperature. All electrolyte components should be nontoxic and environmentally friendly.<sup>[36,43]</sup>

To date, the vast majority of studies that have addressed the topic of organic redox-active materials have been performed in combination with LIB electrodes (with increasing activities for sodium-ion batteries).<sup>[7,8,37,42,44]</sup> As a consequence, a large number of proposed electrolytes for organic active materials are based on well-characterized and optimized LIB solvents. These are mostly linear and cyclic carbonates, such as ethyl methyl carbonate (EMC), dimethyl carbonate (DMC), propylene carbonate (PC), and especially ethylene carbonate (EC).<sup>[45,46]</sup> Because most of these carbonates cannot fulfill all properties required for LIB technology, such as low viscosity, high dielectric constant, and solid/electrolyte interphase (SEI)-forming ability, mixtures of cyclic and linear carbonates are thus applied.<sup>[36]</sup> Therefore, a mixture of EC (which provides a high dielectric constant, but suffers from high viscosity) and DMC (with low viscosity, but a lack of a sufficient dielectric constant) in a ratio of 1:1 is the state-of-the-art solvent for LIBs, and therefore, for organic redox materials.<sup>[47]</sup> However, these solvents suffer from safety problems because they are volatile and flammable.<sup>[42]</sup>

Next, suitable conducting salts for organic redox-active materials need to be selected. Because the applied LIB electrodes demand the presence of  $\text{Li}^+$  ions to store charge through the  $\text{Li}^+$  intercalation process, there is no possibility to use other cations. Accordingly, only lithium salts with versatile anions can be selected. In this regard, anions such as perchlorate ( $\text{ClO}_4^-$ ), tetrafluoroborate ( $\text{BF}_4^-$ ), hexafluoroarsenate ( $\text{AsF}_6^-$ ), and bis(trifluoromethanesulfonyl)imide ( $\text{TFSI}^-$ ) were pro-



posed.<sup>[36,43]</sup> However, by far the most utilized salt is  $\text{LiPF}_6$  because it displays an overall well-balanced series of properties, for example, reasonable ion mobility, degree of dissociation, and SEI-forming abilities.<sup>[36,43]</sup> Considering all of these points, 1 M  $\text{LiPF}_6$  in EC/DME (1:1) is currently adopted as a conventional electrolyte for organic redox-active materials, especially for the half-cell performance evaluation of organic redox materials versus the lithium-metal counter electrode.

The only possibility to overcome the limitations of LIB electrolytes for organic electrodes is to move to other battery concepts, for example, all-organic systems. Because the charge compensation process for all-organic batteries has no direct need for any specific metal ions during the charge/discharge process, a combination of various cations and anions can thus be used as conducting salts.<sup>[8]</sup> Therefore, a larger variety of organic liquid electrolytes should be investigated for these metal-free battery systems.

## 2.2. Ionic-liquid-based electrolytes

ILs have attracted extensive interest as the electrolyte component for LIBs and lithium-metal batteries, owing to their commonly negligible vapor pressure, low flammability, high ionic conductivity, and electrochemical stability.<sup>[31,48–52]</sup> They have also been investigated for batteries based on organic active materials, exhibiting promising properties. In this section, we briefly review the great versatility of ionic-liquid-based electrolytes and their unique roles to suppress the dissolution of organic electrode materials and to enable cycling at high temperatures.

Gurkan et al. used 1-methyl-1-propylpyrrolidinium bis(fluoro-sulfonyl)imide ( $\text{PY}_{13}\text{FSI}$ ) and  $\text{NaFSI}$  as the electrolyte for 2,5-disodium-1,4-benzoquinone.<sup>[53]</sup> The organic redox-active material was immobilized on high-surface-area ordered mesoporous carbon. Compared with standard organic carbonate based electrolytes, substantially improved electrochemical performance, in terms of reversible capacity and cycling stability, were observed for ionic-liquid-based electrolytes. From 22 to 60 °C, the capacity increased from about 150 to 300  $\text{mAh g}^{-1}$  for ionic-liquid-based electrolytes. Moreover, at 60 °C, steady capacity over 300 cycles has been observed. In contrast, at 60 °C, the cell with organic carbonate based electrolytes showed rapid capacity fading during the first 50 cycles due to their poor thermal stability.

As weak polar organic molecules, quinone-based materials often suffer from poor cyclability due to quinone dissolution in aprotic electrolyte (Figure 2). By using  $\text{PY}_{13}\text{TFSI}$  and  $\text{NaTFSI}$  as electrolyte, Wang et al. reported superior capacity retention of calix[4]quinone (C4Q) and 5,7,12,14-pentacenetetrone.<sup>[54]</sup> The inhibited dissolution of these quinones has been correlated to the weaker polarity, lower electron-donor ability, and lower interaction energy of the ILs. As a result, C4Q showed a capacity retention of 99.7% after 300 cycles at a rate of 0.29 C versus a metallic sodium anode. Moreover,  $\text{TFSI}^-$ , with a lower donor number, can better suppress the dissolution of quinones, compared with  $\text{FSI}^-$  anions.

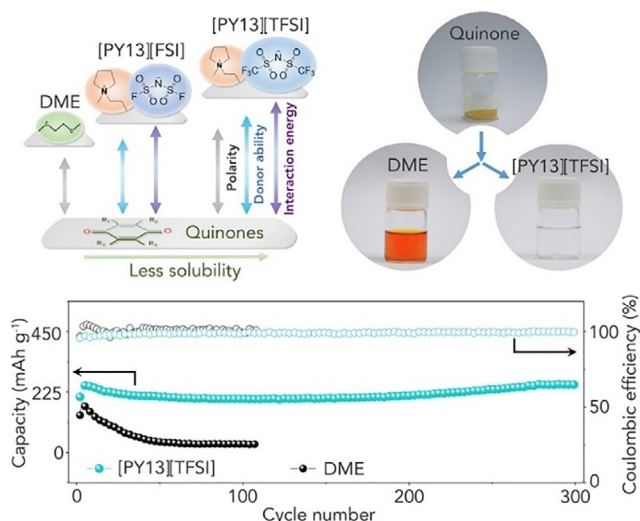


**Figure 2.** Suppressed solubility of quinones in ionic-liquid-based electrolytes as a result of the reduced interaction between the IL and active material. Reproduced from Ref. [54] with permission. Copyright 2019, Elsevier.

Different from the common approach of employing ILs as a “solvent” for the conducting salt, Karlsson et al. reported the use of nonstoichiometric protic ILs as electrolytes for completely metal-free all-organic proton batteries.<sup>[55]</sup> In this case, molecules such as 1,2,4-triazole or 1-methyl-1,2,4-triazole act as a proton acceptor and their protonated derivatives, which are counterbalanced by the  $\text{TFSI}^-$  anion, serve as a proton donor. In other words, the IL acts as a “vehicle” for the proton that is reversibly shuttled between the organic active material, quinone-functionalized poly(3,4-ethylenedioxythiophene) (PEDOT), as schematically illustrated in Figure 3. In addition, the ionic conductivity of such electrolytes is rather high (ca.  $1.2 \text{ S cm}^{-1}$ ) at elevated temperatures, which allows for an excellent rate capability of the organic proton battery. However, the cycling stability remains to be improved, with a capacity retention of only 60% after 100 cycles.

Another approach of employing ILs for metal-free organic batteries has been recently reported by Qin et al.<sup>[56]</sup> The combination of an n-type organic anode and a p-type organic cath-

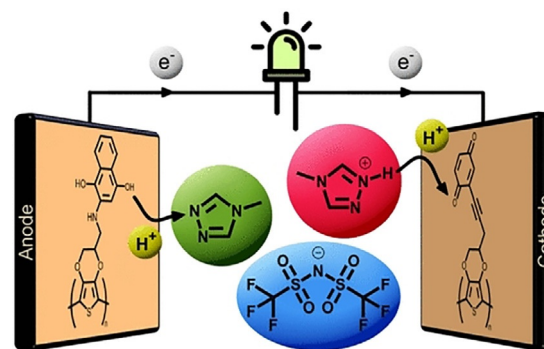


**Figure 3.** Schematic illustration of the working principle of protic ionic-liquid-based electrolytes in all-organic proton batteries. Reproduced from Ref. [55] with permission. Copyright 2018, American Chemical Society.

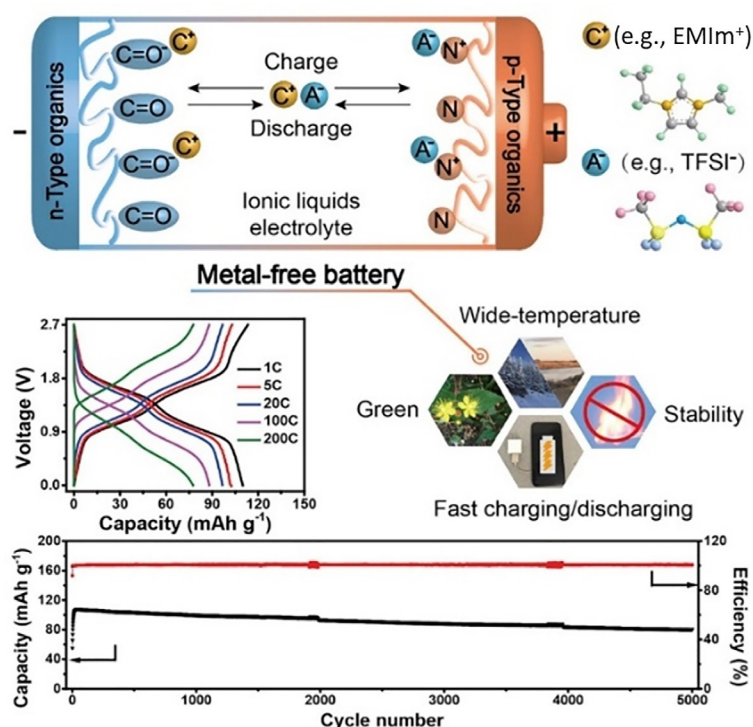


**Figure 4.** Schematic illustration of the general working principle of all-organic batteries based on n-type negative electrodes and p-type positive electrodes, with pure ILs as the electrolyte (e.g., [EMIm][TFSI]). The corresponding voltage profiles, some potential advantages, and the long-term cycling stability of a full cell at a rate of 20 C are also provided. Reproduced from Ref. [56] with permission. Copyright 2019, Elsevier.

ode allows for the use of pure ILs as an “electrolyte,” without any conducting salt. In this configuration, the ionic-liquid anion ( $\text{TFSI}^-$ ) and cation (1-ethyl-3-methylimidazolium,  $\text{EMIm}^+$ ) are actively involved in the charge-storage mechanism and induce the reversible reduction and oxidation of the n- and p-type organic active materials, respectively (Figure 4). Accordingly, such a device might be considered a hybrid between a supercapacitor,<sup>[57–59]</sup> and a dual-ion battery,<sup>[60]</sup> for which the amount of electrolyte used plays a decisive role in the achievable energy density. Interestingly, the essentially pseudocapacitive charge-storage mechanism allows for an excellent rate capability of up to 200 C and highly stable long-term cycling of the full cell (polyimide anode versus polytriphenylamine cathode) for 5000 cycles with a capacity retention of 75% (Figure 4). The potential application of ILs in such batteries might trigger additional fundamental studies on the electrochemistry of organic molecules and polymers in ILs.<sup>[61]</sup>

### 2.3. Polymer electrolytes

It is a straightforward approach to use polymer-based electrolytes for addressing the dissolution issue of organic active materials and for suppressing flammability.<sup>[31]</sup> Initially, gel-type polymer electrolytes were studied, in which a polymer matrix (e.g., poly(vinylidene fluoride-co-hexafluoropropylene), PVdF-HFP) served as a physical host for a standard liquid organic electrolyte, such as  $\text{LiPF}_6$ , in mixtures of organic carbonates.<sup>[62]</sup>

Later, PVdF-HFP copolymer was replaced by a mixture of poly(methacrylate) (PMA) and poly(ethylene glycol) (PEG) to offer satisfactory ionic conductivity (ca.  $1 \text{ mS cm}^{-1}$  at room temperature), because PEG was able to absorb large amounts of liquid electrolyte ( $0.7 \text{ M LiClO}_4$  in DMSO).<sup>[63]</sup> Nevertheless, such an approach does not truly address the solubility issue because there is still a substantial liquid fraction in the electrolyte. Accordingly, DMSO solvent was then replaced by  $\text{SiO}_2$  nanoparticles (7–10 nm) to realize all-solid-state batteries.<sup>[64]</sup> The PMA/PEG- $\text{LiClO}_4$ - $\text{SiO}_2$  (3 wt %) composite showed an optimum ionic conductivity of  $0.26 \text{ mS cm}^{-1}$  at room temperature. By using a pillar[5]quinone ( $\text{C}_{35}\text{H}_{20}\text{O}_{10}$ , P5Q) cathode, a cell voltage of 2.6 V versus a lithium anode and a high initial capacity of  $418 \text{ mAh g}^{-1}$  were achieved. The resulting P5Q/Li cell showed good capacity retention of 94.7% after 50 cycles at a rate of 0.2 C.

Poizot et al. simplified the cell design by using self-standing polymer cathodes, which comprised of an organic active material, tetramethoxy-*p*-benzoquinone (TMQ), conductive carbon, and poly(ethylene oxide) (PEO);  $\text{LiTFSI}$ ; a lithium-metal anode; and a solid electrolyte interlayer of PEO/ $\text{LiTFSI}$  (Figure 5).<sup>[65]</sup> Remarkably, this cell design allows for a reversible capacity of about  $215 \text{ mAh g}^{-1}$  at  $100^\circ\text{C}$ , which is close to the theoretical capacity of TMQ ( $235 \text{ mAh g}^{-1}$ ) and about twice as high as the maximum capacity with a liquid carbonate based electrolyte at  $20^\circ\text{C}$ . In addition, the cycling stability was far superior to that of the reference cell comprising a carbonate-based electrolyte, even though dissolution of the active material could not be fully suppressed, as indicated by the change in color of the PEO/ $\text{LiTFSI}$ -based polymer membrane.

A comparable improvement in cycling stability has been reported by Li et al. for an anthraquinone-based cathode versus a lithium metal anode with a PEO/ $\text{LiTFSI}$ -based electrolyte, containing  $\gamma\text{-LiAlO}_2$  as a ceramic filler and plasticizer.<sup>[66]</sup> The ceramic filler helps to obtain a higher capacity at an elevated temperature of  $65^\circ\text{C}$ . However, it cannot fully prevent dissolution of the active material. Better cycling stability was obtained by using nanosized  $\text{Li}_{0.3}\text{La}_{0.566}\text{TiO}_3$  (LLTO) instead of  $\gamma\text{-LiAlO}_2$ , with a polymerized quinone derivative as an organic active material.<sup>[67]</sup> It was found that the eventual LLTO content had a relatively minor effect on the ionic conductivity. These cells allowed for a remarkable capacity retention of about 90% after 300 cycles. These results suggest effective strategies to overcome the solubility issue of organic active materials.

Fei et al. studied poly(propylene carbonate)- and KFSI-based electrolytes, supported by nonwoven cellulose for organic potassium-metal batteries.<sup>[68]</sup> Despite a rather low ionic conductivity of about  $1.4 \times 10^{-2} \text{ mS cm}^{-1}$ , the resulting cells, incorporating 3,4,9,10-perylene-tetracarboxylic dianhydride (PTCDA) as a cathode, provided a specific capacity of  $118 \text{ mAh g}^{-1}$  at a low current density of  $10 \text{ mA g}^{-1}$ . Remarkably, enhanced cycling stability was observed (Figure 6), compared with a standard carbonate-based liquid electrolyte.

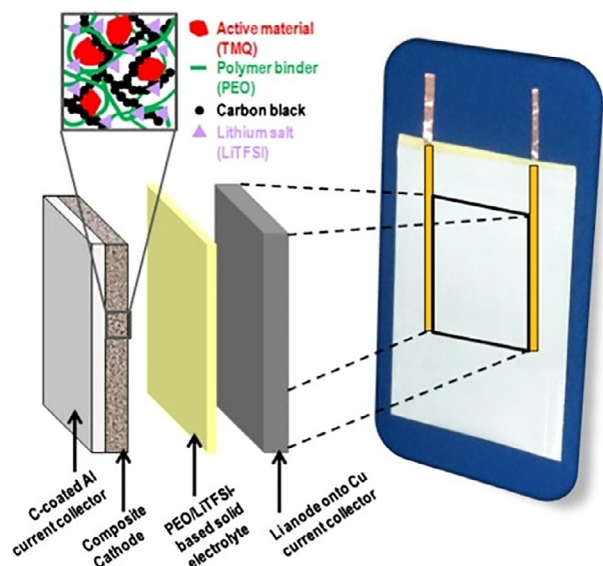


**Figure 5.** Schematic illustration of the organic lithium polymer battery. Reproduced from Ref. [65] with permission. Copyright 2015, Elsevier.

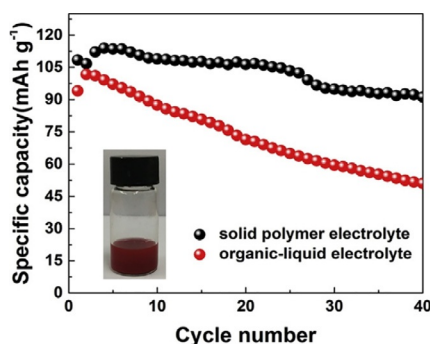


**Figure 6.** Cycling stability of a PTCDA/K cell at  $20 \text{ mA g}^{-1}$  with a poly(propylene carbonate)- and KFSI-based electrolyte (black), in comparison with a cell comprising KFSI in a 1:1 EC/DEC (red). Inset: the dissolution of PTCDA in the carbonate-based electrolyte. Reproduced from Ref. [68] with permission. Copyright 2018, Elsevier.

Studies on polymer-based electrolytes for organic active material based batteries are still rare, but are promising strategies to overcome the solubility issue of organic active materials, especially for small molecules. Further improvement is still needed.

## 2.4. Recent progress in the use of concentrated electrolytes

The dissolution of organic active materials into the organic-solvent-based electrolyte of the battery system is a well-known drawback and leads to reduced cycle life, especially if small molecules, such as carbonyls, are exploited as energy-storage materials.<sup>[47,69]</sup> Several approaches to reduce this dissolution have been proposed, such as cross-linking,<sup>[70]</sup> attachment of side groups that change the polarity of the active materials,<sup>[47]</sup> and polymerization.<sup>[71]</sup> However, these attempts lead to an increase in the molar mass of the active materials used, and therefore, a decrease in the gravimetric capacity. Another ap-

proach is to use concentrated electrolytes, which bear high concentrations of conducting salts ( $> 1 \text{ M}$ ); these have several advantages.<sup>[47,72]</sup> 1) The increased salt concentration in the electrolyte could suppress the ability of the solvent used to dissolve organic active materials of the electrodes. 2) The increase in salt concentration increases the viscosity of the electrolyte, which also kinetically reduces the dissolution rate of active materials. 3) Solvent-deficient electrolytes can reduce the undesired oxidation of solvents and side reactions, enhance the thermal stability, and suppress the flammability (flash point) of organic solvents.

In this regard, Chen et al. investigated the beneficial effect of highly concentrated electrolytes on an anthraquinone organic active material.<sup>[73]</sup> In previous studies, it was shown that ether-based solvents could dissolve large amounts of conductive salts and suppress the dissolution of active material in sulfur-based batteries.<sup>[74]</sup> In their work, Chen et al. proved the same concept for a 9,10-anthraquinone cathode material in a sodium battery, for which they used sodium trifluoromethane sulfonate (NaTFS) salt with concentrations up to  $4 \text{ M}$  in triethylene glycol dimethyl ether (TEGDME), which displayed a viscosity of  $97 \text{ mPa s}$  and a conductivity of  $0.79 \text{ mS cm}^{-1}$  at  $25^\circ\text{C}$ .<sup>[73]</sup> In this specific system, the highly concentrated  $4 \text{ M}$  electrolyte displayed a better cycling performance than that of the others, with a high coulombic efficiency near  $100\%$  (instead of  $\approx 88\%$  in  $1 \text{ M}$  solution), the highest initial specific capacity of  $208 \text{ mAh g}^{-1}$  at  $0.2 \text{ C}$  (compared to only about  $160 \text{ mAh g}^{-1}$  in  $1 \text{ M}$  electrolyte) and a better capacity retention of  $88\%$  after 50 cycles (compared with about  $50\%$  for the  $1 \text{ M}$  electrolyte; Figure 7).

Another example of improved cycling stability in highly concentrated systems is the use of tannic acid (TA) as an organic anode material for LIBs.<sup>[75]</sup> In typical LIB electrolytes (e.g.,  $1 \text{ M}$

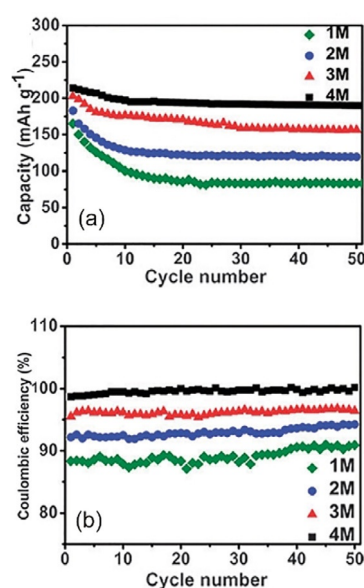


**Figure 7.** a) Cycling stability and b) coulombic efficiency of 9,10-anthraquinone in 1, 2, 3, and  $4 \text{ M}$  NaTFS in TEGDME. Reproduced from Ref. [73] with permission. Copyright 2015, Wiley.



LiPF<sub>6</sub> in EC/DEC), TA dissolves rather fast, and thus, limits the cycle life of the electrochemical cell. To overcome this limitation, high concentrations of LiTFSI salt (1, 3, and 5 M) in the same solvent, EC/DEC, can be used.<sup>[75]</sup> Although large amounts of salt in this system reduce the initial specific capacity, a very stable cycling capacity of 110 mAh g<sup>-1</sup> over 250 cycles is achieved in the 5 M electrolyte. In the meantime, TA loses 45 % of its initial capacity in 1 M LiTFSI and 75 % in 1 M LiPF<sub>6</sub> (the capacity decays to below 50 mAh g<sup>-1</sup> after 100 cycles).

The loss in cycle life is related to the very prominent self-discharge of organic active materials. This phenomenon is often caused by the dissolution of active redox material. One example for this is poly(2,2,6,6-tetramethylpiperidiny-1-oxymethacrylate) (PTMA), for which the self-discharge process is caused by a shuttle effect of dissolved redox-active moieties in the electrolyte.<sup>[76]</sup> Recently, it has been shown that the increase in the concentration of 1-butyl-1-methylpyrrolidinium tetrafluoroborate (Py<sub>14</sub>BF<sub>4</sub>) in PC (1, 2, and 3 M) retards the self-discharge of PTMA (Figure 8),<sup>[77]</sup> which can be explained by a decreased dissolution of organic redox groups in the concentrated electrolyte. This inhibits capacity loss during cycling, as well as self-discharge, by the proposed shuttle effect. However, a reduced specific capacity was found for PTMA if it was used in highly concentrated systems. This is caused by a decrease in ion mobility and an inhibition of the wetting of the electrode surface.<sup>[78]</sup>

The above-discussed examples clearly emphasize the beneficial effect of highly concentrated systems, in terms of cycling stability and self-discharge behavior. Nevertheless, in practical systems, a proper electrolyte concentration should be studied to provide reasonable cycling stability and accessible specific capacity.

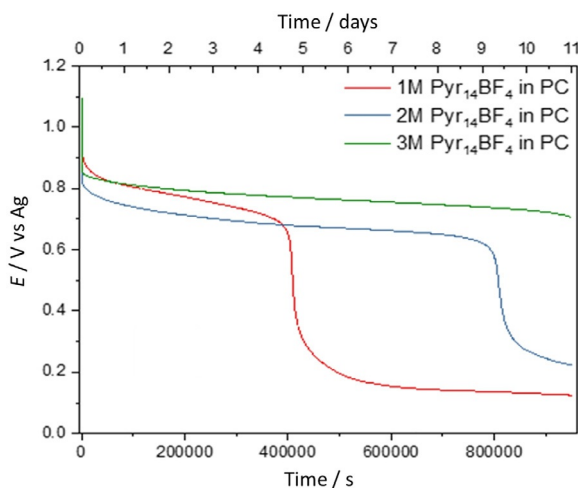


**Figure 8.** Voltage excursion of PTMA during 11 days of self-discharge tests in 1, 2 and 3 M Py<sub>14</sub>BF<sub>4</sub> in PC. 1 M loses all charge after 5 days, 2 M after 9 days, 3 M is able to deliver residual charge after 11 days of self-discharge. Reproduced from Ref. [77] with permission. Copyright 2019, Wiley.

## 2.5. Recent progress in the use of aqueous electrolytes

To overcome the limitations of traditional organic carbonate based LIBs, safe and environmentally friendly aqueous electrolytes have been widely investigated.<sup>[79–82]</sup> Dahn and Wainwright first reported aqueous LIBs in 1994 by using a 5 M aqueous solution of LiNO<sub>3</sub>, which showed a higher energy density than that of lead–acid batteries.<sup>[83]</sup> The ionic conductivity of aqueous electrolytes is typically higher than that of organic-solvent-based electrolytes by two orders of magnitude, resulting in good rate and power performance.<sup>[84]</sup>

Electrode materials with charge-storage potentials within the ESW of aqueous electrolytes can be used,<sup>[85]</sup> leading to a relatively low cell voltage. Organic electrodes, such as polytriphenylamine, have a high operating potential of 3.9 V versus Li<sup>+</sup>/Li,<sup>[86]</sup> which is close to that for LiCoO<sub>2</sub> and LiMn<sub>2</sub>O<sub>4</sub>, and is promising to maximize the cell voltage. However, in neutral aqueous electrolytes, parasitic O<sub>2</sub> evolution reactions occur during continued charging due to the adsorption of H<sub>2</sub>O on the surface of the polytriphenylamine electrode.

To suppress the side reactions of water splitting, a previously reported “water-in-salt” electrolyte of 21 m (m = mol kg<sup>-1</sup><sub>water</sub>) LiTFSI for inorganic intercalation materials<sup>[87]</sup> has been adopted for an all-organic battery.<sup>[86]</sup> The water molecules are bound by the salt, and the electrochemical activity of water is substantially suppressed. Concentrated aqueous electrolytes were further developed to extend the ESW to 1.83–4.9 V versus Li<sup>+</sup>/Li by using a “water-in-bisalt” electrolyte,<sup>[88]</sup> and to 1.25–5.05 V versus Li<sup>+</sup>/Li by using a Li(TFSI)<sub>0.7</sub>[N(SO<sub>2</sub>C<sub>2</sub>F<sub>5</sub>)<sub>2</sub>]<sub>0.3</sub>·2H<sub>2</sub>O hydrate-melt electrolyte.<sup>[89]</sup> At potentials below 1.2 V versus Li<sup>+</sup>/Li, a dramatic increase in the repulsion between the anode surface and the anions (TFSI<sup>-</sup>, trifluoromethane sulfonate (OTf<sup>-</sup>)), as revealed by molecular dynamics simulations, precludes the approach of anions on the anode surface, and consequently, prefers water adsorption.<sup>[90]</sup>

Quinones, as sustainable electrode materials, often show unwanted dissolution in aprotic electrolytes, resulting in detrimental shuttle effects, fast capacity decay, and short service life.<sup>[91]</sup> Compared with the strategies targeting modification of the electrode to stabilize the organic materials, or the introduction of specific separators to prevent such shuttling of the dissolved species,<sup>[14]</sup> Yao and co-workers demonstrated that aqueous electrolytes permitted the widespread applicability of quinone-based anode materials, such as pyrene-4,5,9,10-tetraone and its polymerized version, versus industrially established cathodes, and thus, exhibited excellent aqueous cycling stability for up to 3000 cycles and very low water solubility (ca. 10<sup>-6</sup> M).<sup>[28]</sup>

## 3. Organic Materials as Redox Electrolytes for Flow Batteries

Unlike organic solid electrodes, for RFBs, the organic species are dissolved in supporting electrolytes, including solvents and conducting ions. Accordingly, general solution properties, such as viscosity, ionic conductivity, and freezing and boiling points, as well as key performance-determining properties, such as the

solubility of active organic compounds, the ESW of liquid electrolytes, chemical stability, and electrochemical reversibility of the organic species, need to be considered for formulating the electrolytes.<sup>[26]</sup> A high volumetric energy density of the RFBs requires a large redox potential gap of the active species in the anolyte and catholyte, high solubility, and preferably a multi-electron-transfer reaction for the active materials, whereas a good power performance requires fast diffusion of the organic redox species in the solvent and fast reaction kinetics at the electrode surface. In this section, we discuss the features and rational design of redox fluidic electrolytes that use organic materials as the active components. For a contradistinctive study, the supporting media are discussed in the same order as that presented in Section 2.

### 3.1. Organic solvents

RFBs utilizing organic-solvent-based electrolytes were first proposed by Matsuda et al. in 1988,<sup>[92]</sup> containing a metal complex, tris(bipyridine)ruthenium(II) ([Ru(bpy)<sub>3</sub>]<sup>2+</sup>), in acetonitrile. A high open-circuit voltage of 2.6 V has been observed. In 2011, Li et al. proposed a RFB by using all-organic redox species, with 2,2,6,6-tetramethylpiperidine 1-oxyl (TEMPO) and *N*-methylphthalimide in acetonitrile, and a NaClO<sub>4</sub> salt.<sup>[93]</sup> The flow cell tests showed a low coulombic efficiency of about 90%. Next, a hybrid metal-organic RFB was developed with a lithium-metal anode and an anthraquinone-based active catholyte material, with LiPF<sub>6</sub> in PC.<sup>[94]</sup> This earlier work demonstrated high-voltage RFBs (>2 V) with organic active materials, which were enabled by using organic solvents. Later, low-molecular-weight organic materials were studied; these are more favorable in terms of costs and solubility.<sup>[95]</sup>

However, many organic-solvent-based RFBs suffer from rather low operating current densities (<10 mA cm<sup>-2</sup>). In addition, ion-exchange membranes showed relatively poor conductivity in organic-solvent-based electrolytes, leading to a low power output.<sup>[96]</sup> Microporous separators that can conduct charge carriers fast and avoid the crossover of active materials through a size-exclusion effect are preferred in such cases, as discussed in Section 3.3.

Conducting salts containing tetraalkylammonium cations and BF<sub>4</sub><sup>-</sup>, ClO<sub>4</sub><sup>-</sup>, PF<sub>6</sub><sup>-</sup>, and TFSI<sup>-</sup> anions are often used in organic solvents.<sup>[97]</sup> Apart from their role as charge carriers, it was also found that they might interfere with electrochemical reactions and the chemical stability of organic active species.<sup>[96]</sup> Furthermore, a compatibility issue between the organic radicals and organic solvents was also found.

The solubility of many organic redox materials in organic solvents is often limited, which is insufficient for use as electrolytes for RFBs. For instance, 2,5-di-*tert*-butyl-1,4-bis(2-methoxyethoxy)benzene (DBBB),<sup>[98]</sup> which is known as a redox shuttle molecule for overcharging protection in LIBs,<sup>[99,100]</sup> shows a solubility of about 0.4 M in carbonates.<sup>[101]</sup> PEO chains of different lengths have been incorporated into the DBBB motif, which results in liquid organic redox-active materials at room temperature.<sup>[101]</sup> Such liquid redox materials can work as cosolvents for the conducting salts. Additional organic solvent, such as

acetonitrile has been used to reduce the overall viscosity,<sup>[102]</sup> by sacrificing the volumetric capacity of the electrolytes. However, practical demonstrations of flow cell performance are only at very low current densities.<sup>[103]</sup> In addition, the pressure drop and pumping losses need to be considered for viscous electrolytes.

### 3.2. Ionic liquids (ILs)

The use of ILs in flow battery electrolytes arises from the assumption that high energy density can be realized because of the possibility of elevating the cell voltage far beyond that of aqueous electrolytes.<sup>[35]</sup> In addition, ILs may provide broad temperature adaptability due to their high thermal stability, low volatility, and often nonflammability. ILs have been used as active components,<sup>[104–106]</sup> reaction media,<sup>[107,108]</sup> additives,<sup>[109,110]</sup> and redox mediators<sup>[111]</sup> for redox-active species. If the redox species are part of the anion or cation of the ILs, a high effective concentration can be obtained for energy-rich electrolytes. For instance, TEMPO and anthraquinone derivatives as redox-active counteranions have been incorporated into poly(IL)s for RFBs.<sup>[112]</sup>

Different from aqueous electrolytes, different reaction mechanisms, solubility, and reaction kinetics<sup>[113]</sup> of redox species can be obtained in ILs. Side reactions related to water molecules, such as hydrolysis and hydroxylation reactions, can be avoided. The formation of complexes,<sup>[107]</sup> a change in the coordination environment, and enhanced intermolecular interactions between the redox species and constituent ions of the ILs in electrolytes may be responsible for the distinct physio- and electrochemical properties. Depending on the absence/presence of a proton donor/acceptor in [BMIm][BF<sub>4</sub>] and [BMIm][PF<sub>6</sub>] (BMIm = 1-butyl-3-methylimidazolium), benzoquinone and hydroquinone showed different electron-transfer mechanisms, with or without the involvement of (de)protonation.<sup>[114]</sup> This character is important in the case of the chemical instability of organic materials, which are associated with water attack. *para*-Benzoquinone, which is insoluble in water, exhibits a significant solubility of 0.4 M and reversible electrochemical redox reaction in [Py<sub>14</sub>][TFSI].<sup>[115]</sup> An all-organic flow battery containing benzophenone and 1,4-di-*tert*-butyl-2,5-dimethoxybenzene in acetonitrile (0.01 M active species) with [TEA][TFSI] (TEA = tetraethylammonium) as the supporting salt was tested by using a microporous separator.<sup>[116]</sup> Despite a high open-cell voltage of 2.95 V, the cell showed a low energy efficiency of only 44% at 1 mA cm<sup>-2</sup>. In addition, continuous capacity fading was observed over 50 charge/discharge cycles.

Metal complexes with organic ligands are promising for improving the energy density by utilizing multielectron reactions.<sup>[107,117,118]</sup> However, insufficient solubility (typically <0.1 M) of these organometallic compounds in ILs and poor electrochemical reversibility restrict their applications. In addition, ILs as supporting electrolytes with a large complex cation and anion may cause difficulties in the selection of ion-exchange membranes to quickly conduct charge carriers, which is often a limiting factor towards a high operating current density. Other issues, such as high viscosity (>100 mPa s) and poor



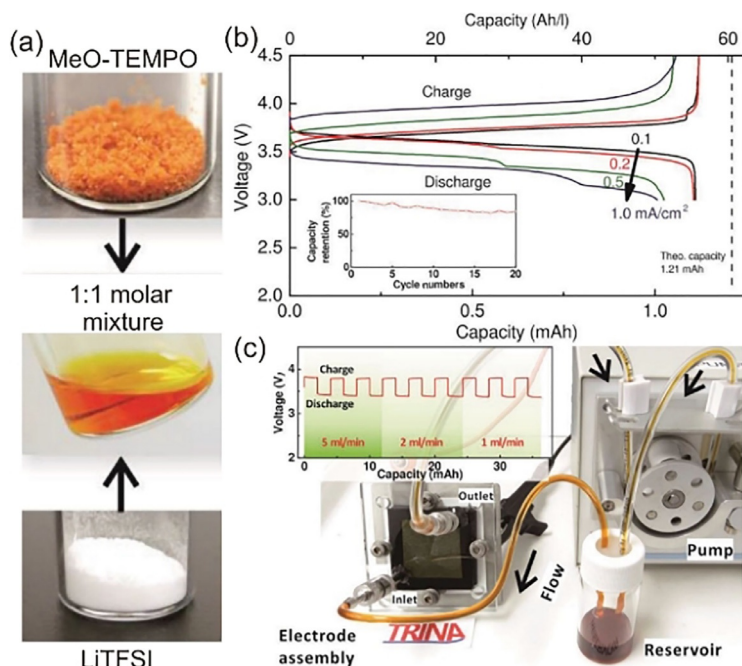


**Figure 9.** a) The formation of a liquid mixture of 4-methoxy-TEMPO and LiTFSI (MTLT; 1:1) at room temperature. b) Voltage profiles and cycling stability of a static cell with a catholyte consisting of MTLT + 17 wt% H<sub>2</sub>O versus a Li anode. c) The corresponding flow cell setup and charge/discharge behavior. Reproduced from Ref. [102] with permission. Copyright 2015, Wiley.

ionic conductivity ( $<1 \text{ mS cm}^{-1}$ ) of typical room-temperature ILs, further hinder the utilization of ILs for flow systems, making them unattractive.

In addition to traditional ILs as supporting electrolytes, “solvate ILs,”<sup>[119]</sup> consisting of complex ions (i.e., solvates,  $[\text{Li-4-methoxy-TEMPO}]^+$ ) and their counterions ( $\text{TFSI}^-$ ) in a molten state (Figure 9a), have been explored as a highly concentrated catholyte for a hybrid RFB.<sup>[102]</sup> It was considered that an ordered ionic structure formed with contacted ion pairs due to strong interactions between the  $\text{Li}^+$  ions and the  $\text{N-O}^+$  sites of the organic radicals. A lithium-ion-conducting ceramic separator was used for the assembly of a hybrid flow cell with a lithium-metal anode. Certain amounts of water (17 wt%) were added to the organic radical catholyte to reduce the viscosity. The proof-of-concept was demonstrated under static conditions at current densities below  $1 \text{ mA cm}^{-2}$  (Figure 9b) and under flow conditions with capacity control (Figure 9c).

Recently, the concept of “water-in-ILs” by using hydrophilic ILs and a small halide anion (such as imidazolium chloride and ammonium chloride) makes it possible for the effective use of ILs for RFBs.<sup>[113,120]</sup> A good flowability (viscosity  $<10 \text{ mPa s}$ ) and high ionic conductivity ( $>10 \text{ mS cm}^{-1}$ ) have been obtained, which are superior to those of common organic solvents and room-temperature ILs. Meanwhile, a broad ESW (ca. 3 V; Figure 10a) for water-in-ILs has been observed, which is suitable for most reported organic redox couples.<sup>[26]</sup> It was found that such supporting electrolytes allowed access to the low negative redox potentials ( $-0.2$  to  $-1.6 \text{ V}$  vs. Ag) of metal phthalocyanines in aqueous media. Thus, the selection space of redox-

active molecules in aqueous electrolytes can be largely extended without the involvement of the hydrogen evolution reaction. Additionally, as supporting electrolytes, the mixture of water and ILs can extend the temperature stability window. An aqueous flow cell operating at  $-32^\circ\text{C}$  has been demonstrated by using metal phthalocyanine and iron redox pairs (Figure 10b).<sup>[121]</sup> Importantly, the solubility limit of organic molecules can be extended in the proposed supporting electrolyte, such as 6 M 2-methoxyhydroquinone in 10 M [BMIm]Cl/H<sub>2</sub>O, in contrast to 1.8 M in pure water,<sup>[122]</sup> and 4.3 M 4-hydroxy-TEMPO in 3 M [BMIm]Cl/H<sub>2</sub>O, compared with 2.1 M in pure water,<sup>[123]</sup> arising from enhanced molecular interactions between the  $\text{BMIm}^+$  cations and organic molecules.

By utilizing the different solubilities of organic molecules in water and in hydrophobic ILs (Figure 11a), a liquid-liquid biphasic electrolyte system without the use of a membrane has been designed (Figure 11b,c).<sup>[124]</sup> The thermodynamic equilibrium of the two phases is governed by the partition coefficients. Flow cell tests were performed with a low concentration of quinones ( $<0.1 \text{ M}$ ) and a low current density ( $<0.5 \text{ mA cm}^{-2}$ ). Slope charge/discharge curves were observed with a high coulombic efficiency, similar to those of membrane-based systems. The overall cell performance is limited from the anolyte side containing IL with high viscosity (83 mPa s) and low ionic

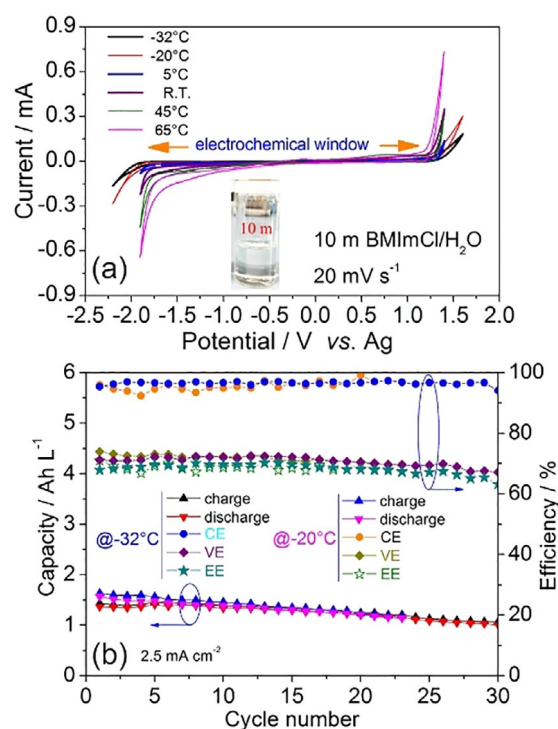


**Figure 10.** a) ESW as a function of the temperature of 10 M [BMIm]Cl/H<sub>2</sub>O supporting electrolyte. b) Redox flow cell tests at  $-32$  and  $-20^\circ\text{C}$  by using Ni phthalocyanine anolyte and  $\text{FeCl}_2$  catholyte. CE = coulombic efficiency, VE = voltage efficiency, EE = energy efficiency. Reproduced from Ref. [121] with permission. Copyright 2019, American Chemical Society.

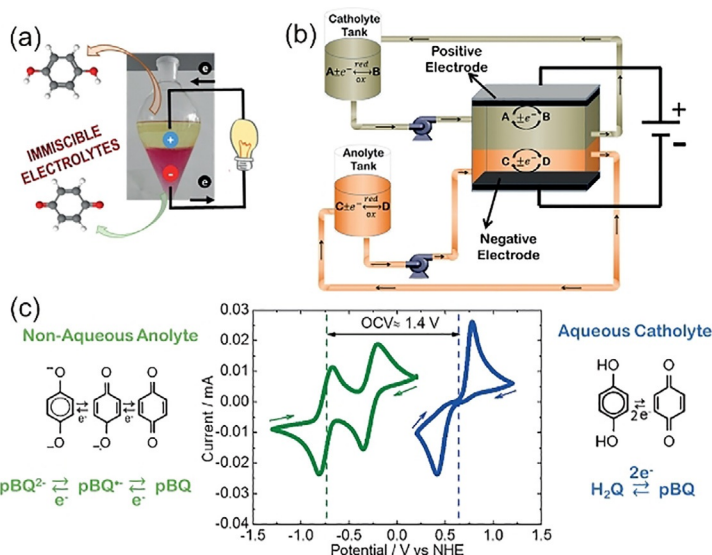


**Figure 11.** a) A membrane-free concept of using immiscible redox electrolytes. b) Flow cell with a horizontal design. c) Cyclic voltammetry curves of the nonaqueous anolyte (parabenzquinone in [Py<sub>14</sub>][TFSI]) and aqueous catholyte (hydroquinone in aqueous HCl). Reproduced from Ref. [124] with permission. Copyright 2017, Wiley.

conductivity (2.2 mS cm<sup>-1</sup>). Self-discharge due to the contact of redox pairs at the liquid/liquid interface and cross-mixing of active species through the interface are issues that remain to be solved in the future.

### 3.3. Redox-active polymers

Unlike the batteries discussed in Section 2 with solid electrode materials and porous separators, RFBs with liquid redox electrolytes require high-performance membranes to avoid solution mixing. It is one of the key factors for the successful operation of RFBs. However, to date, commercially available membranes for RFBs are rather limited.<sup>[125]</sup> Unwanted high permeability of active species through the membranes will eventually lead to failure during long-term cycling. Additionally, the compatibility issue between ion-exchange membranes and redox electrolytes must be considered. To tackle these issues, new design strategies for materials have been developed.

Compared with small organic molecules for RFBs, the use of redox-active polymers, with redox pendants, such as TEMPO,<sup>[126]</sup> dimethoxybenzene, viologen, and cyclopropenium ions,<sup>[127]</sup> has advantages, such as 1) possible replacement of expensive and poorly performing ion-exchange membranes with low-cost, porous, size-exclusion membranes,<sup>[128]</sup> and 2) effective inhibition of the migration of redox species between electrode compartments during battery cycling. The development of a new generation of size-exclusion RFBs is promising in terms of costs and reliability. Charge transport may occur through electron hopping between neighboring redox units of the pendant groups, through the polymer backbones, or by using small redox shuttle molecules.<sup>[129]</sup> Such long-distance intraparticle charge transfer requires high charge mobility. Furthermore, it was found that the electroactivity and reversibility depended on the length of the tether groups.<sup>[127]</sup> Low-cost

(less than \$200 per ton) and environmentally friendly biopolymers of lignin derivatives, bearing phenol groups, have recently been proposed as flow battery electrolytes,<sup>[130]</sup> which is rather attractive towards inexpensive, large-scale energy storage.

Nevertheless, some implementation challenges remain for the utilization of redox-active polymers. A high viscosity of 50 mPa s at 25 °C was observed at a concentration of only 0.1 M for liginosulfonate in perchloric acid.<sup>[130]</sup> Polymer solutions with a concentration of up to 1 M showed a reduced diffusion coefficient, and hence, reduced current at an electrode.<sup>[131]</sup> Additionally, charge trapping<sup>[132]</sup> and adsorption of polymer species onto the electrodes can impede effective operation and even clog the flow channels of flow batteries.<sup>[133,134]</sup>

As opposed to redox polymers, redox-active oligomers with tunable molecular dimensions, paired with microporous polymer membranes with pore sizes smaller than that of the hydrodynamic radii of the redox oligomers, have been reported to facilitate charge and mass transfer.<sup>[133,135]</sup> Chemical cross-linking can be used to restrict pore swelling and to control the pore size of the polymer separators. By using membranes composed of polymers with intrinsic microporosity (PIMs), crossover-free flow batteries may be realized.<sup>[133,136]</sup>

In addition, the use of cross-linked and dispersible polymer colloids<sup>[137]</sup> and particulate slurry electrolytes,<sup>[138]</sup> instead of soluble organic polymers,<sup>[131,139]</sup> may reduce the viscosity due to weak interactions between particulates and solvent molecules, and break the solubility limit of active materials. Despite the novelty and merits discussed above, the successful operation of these all-polymer RFBs remains challenging.<sup>[140]</sup>

### 3.4. Aqueous systems

Early studies on aqueous RFBs with hybrid organic and inorganic active materials were reported in 2009.<sup>[141]</sup> Later, Aziz et al. demonstrated a high-performance, metal-free organic/inorganic RFB in acidic aqueous electrolyte.<sup>[142]</sup> 9,10-Anthraquinone-2,7-disulfonic acid and Br<sub>2</sub>/Br<sup>-</sup> as redox pairs showed a high peak power density of 0.6 W cm<sup>-2</sup> at 1.3 A cm<sup>-2</sup>, owing to a rapid electron-transfer reaction of the redox species<sup>[142]</sup> and a high conductivity of the electrolyte and membrane.<sup>[143]</sup> Quinones are known redox species. Narayanan et al. studied an aqueous RFB with all-quinone-based active materials for the anolyte and catholyte.<sup>[144]</sup> Anthraquinones, which can be exploited from waste products of the pulp industry, are promising for largely reducing the costs of materials compared with the state-of-the-art vanadium electrolyte.<sup>[142,144–146]</sup>

To replace toxic bromine,<sup>[142]</sup> Aziz et al. reported a nontoxic ferrocyanide paired with anthraquinone derivatives in less corrosive alkali electrolyte.<sup>[147]</sup> This led to a decrease in the crossover rate of active materials, costs, and corrosion issues. The cell voltage was further increased by pairing ferrocyanide with 2,5-dihydroxy-1,4-benzoquinone (DHBQ) as the anolyte active material, which had a low reduction potential of -0.72 V

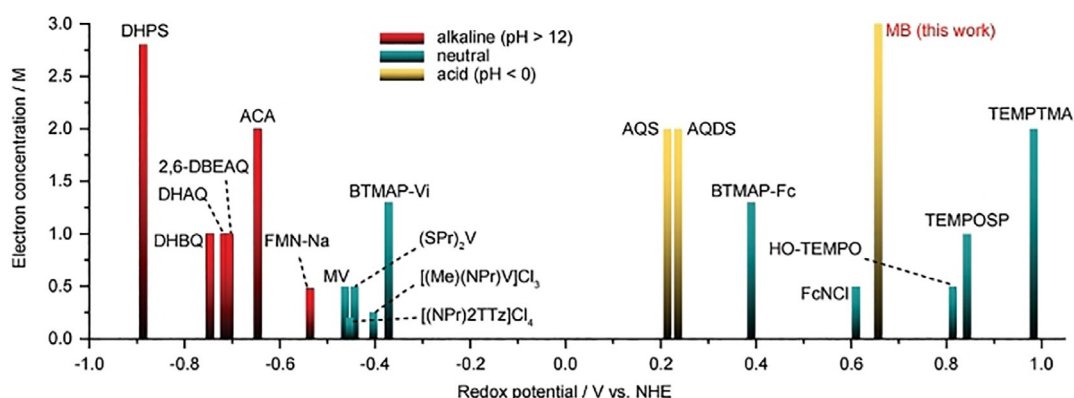


**Figure 12.** Redox potential and effective electron concentration of representative organic materials in aqueous electrolytes of different pH values. DHPS = 7,8-dihydroxyphenazine-2-sulfonic acid, DHAQ = 2,6-dihydroxyanthraquinone, 2,6-DBEAQ = 4,4'-((9,10-anthraquinone-2,6-diyl)dioxy)dibutylate, ACA = 7/8-carboxylic acid, FMN-Na = flavin mononucleotide, MV = methyl viologen, (SPR)<sub>2</sub>V = 1,1'-bis[3-sulfonatopropyl]-4,4'-bipyridinium, [(NPr)2TTz] = 4,4'-[thiazolo[5,4-d]thiazole-2,5-diyl]bis(1-(3-(trimethylammonio) propyl)pyridin-1-ium) tetrachloride, [(Me)(NPr)V]Cl<sub>3</sub> = 1-methyl-10-[3-(trimethylammonio)propyl]-4,40-bipyridinium tri-chloride, BTMAP-VI = bis(3-(trimethylammonio)propyl)viologen tetrachloride, AQS = anthraquinone-2-sulfonic acid, AQDS = 9,10-anthraquinone-2,7-disulfonic acid, BTMAP-Fc = bis((3-(trimethylammonio)propyl)ferrocene) dichloride, HO-TEMPO = 4-hydroxy-TEMPO, MB = methylene blue, TEMPOSP = TEMPO-4-sulfate potassium salt, TEMPTMA = *N,N,N*-2,2,6,6-heptamethylpiperidinyloxy-4-ammonium chloride. Reproduced from Ref. [150] with permission. Copyright 2019, Wiley.

versus a standard hydrogen electrode (SHE).<sup>[148]</sup> Moreover, reduced nucleophilic attack of DHBQ by water and OH<sup>−</sup> was expected, leading to good chemical resistance. Recently, the alkali RFB was further studied by exploring a new class of alloxazine derivatives as anolyte active materials by Aziz et al.,<sup>[149]</sup> which was important to enrich the organic material candidates. These materials exhibited excellent cycling stability over 400 cycles (a capacity fading of 0.02% per cycle) versus ferrocyanide.

The redox potentials of organic materials are mostly determined by their types, molecular structures, and functional groups.<sup>[150,151]</sup> In addition, in aqueous electrolytes, the change in pH value may cause a shift in the thermodynamic redox potentials of proton-related reactions (such as that for quinones).<sup>[27,146,150,152]</sup> Mostly, organic materials can only be used within certain pH ranges (Figure 12), which leads to difficulties in combining redox pairs to maximize the cell voltage and their concentrations. In general, the solubility of organic materials in aqueous systems can be improved by structurally introducing hydrophilic groups, such as hydroxy, ammonium, sulfate, and phosphate.<sup>[142,144,153–155]</sup> Computational screening has proven to be a powerful method to determine their derivatives,<sup>[156]</sup> with improved cycling stability and fast electron-transfer rate.<sup>[157]</sup>

Yu et al. recently explored a class of heteroaromatic phenothiazine derivatives (for instance, MB (Figure 7)) in acidic catholyte, which exhibited a high electron concentration of 3 M and excellent chemical stability.<sup>[150]</sup> A high electrolyte utilization of about 87% and a steady cycling stability (a capacity fading of 0.074% per cycle) at 80 mA cm<sup>−2</sup> have been observed for a concentrated catholyte of 1.5 M MB (two-electron reaction materials).

Generally, ion-exchange membranes show good ionic conductivity at low or high pH, but poor ionic conductivity in neutral aqueous electrolytes.<sup>[110,142,150]</sup> This is also an important

factor that should be considered in the combination of active materials with membranes.

## 4. Summary and Outlook

The use of organic redox-active materials, containing abundant elements, such as hydrogen, nitrogen, carbon, and oxygen, is attracting increasing attention for the development of rechargeable batteries. To promote their utilization as either traditional solid-state electrode materials for LIBs or dissolved fluidic redox species in liquid catholytes and anolytes for RFBs, it is of great importance to explore better performing electrolytes towards the realization of safe batteries,<sup>[31]</sup> with improved cycling stability, high round-trip efficiency, and suitable energy and power densities. Herein, by surveying representative examples of different organic active materials and electrolyte components, we discussed the performance-limiting scenarios and highlighted some recent illuminating improvements for new electrolyte formulations.

Despite the use of different system architectures for LIBs and RFBs (Figure 1), they have some common requirements for a given electrolyte (Figure 13), including safety; wide ESW; fast ion transport; broad temperature adaptability; long-term cycling stability; and high efficiency, that is, minimized side reactions. From a performance point of view, nonaqueous electrolytes dominate state-of-the-art LIBs, whereas aqueous electrolytes prevail for RFBs.

Depending on the number of ions present in the given solvent (Figure 13), concentrated electrolyte,<sup>[158]</sup> water-in-salt electrolyte,<sup>[87,88]</sup> and water-in-IL<sup>[113,120,121]</sup> concepts have been developed. If the ions outnumber the water molecules in the electrolyte, the ESW of water-based systems can be largely extended (Figure 14).<sup>[87,88,113,120,121]</sup> In addition, the cycling stability of the organic redox materials in these concentrated electrolytes can be improved due to the inhibition of chemical attack



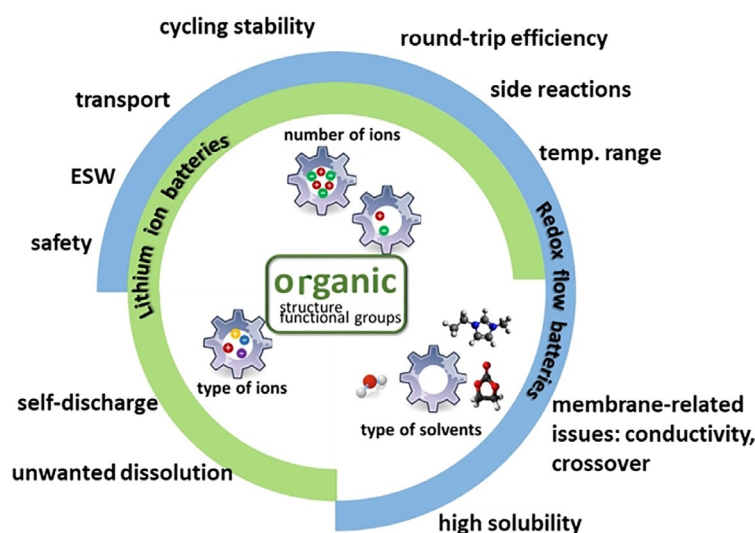


**Figure 13.** A wraparound overview of the components and functions of electrolytes that affect the physio- and electrochemical properties of organic energy-storage materials for LIBs and RFBs, highlighting common issues and differences.

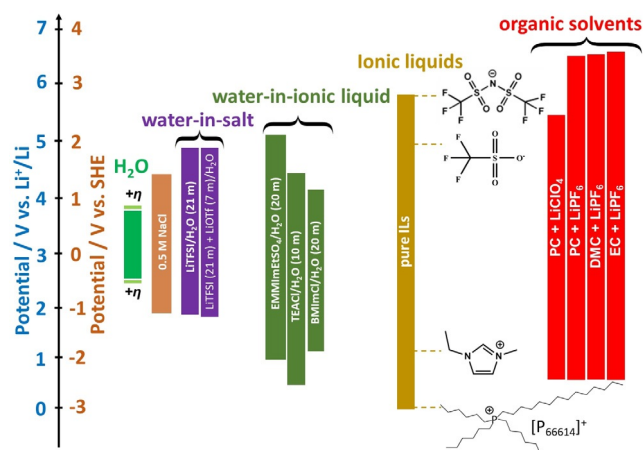


**Figure 14.** A comparison of the ESW of different solvents and supporting electrolytes.<sup>[87, 88, 113, 120, 121, 158–160]</sup> EMIm = 1-ethyl-2,3-dimethylimidazolium.

by solvent molecules with largely reduced content. Furthermore, different solvation models, molecular and ionic coordination environments, and molecular interactions can affect the dissolution behavior and possible side reactions with organic active materials. Interestingly, water-deficient electrolytes, as shown in Figure 14, allow for a combination of a wide range of organic redox species with a large redox potential gap. The cathodic and anodic stability boundary can be significantly shifted (Figure 14). Compared with water-in-salt electrolytes,<sup>[87, 88]</sup> water-in-IL electrolytes allow for the lower boundary, in particular, to be extended to even lower potentials.<sup>[113, 120, 121]</sup> They are promising as alternatives to flammable organic solvents<sup>[159]</sup> and viscous ILs, enabling a moderate cell voltage of about 2 to 3 V.<sup>[160]</sup>

Different types of conducting ions and solvents allow for the realization of tunable physio- and electrochemical properties. They play a critical role in the safety,<sup>[31]</sup> accessible capacity, rate

performance, and long-term durability. An optimized combination of organic active materials, solvents, and conducting ions appears to be key in this regard, considering also other specific requirements, such as membrane-related issues for RFBs.<sup>[161]</sup> Although self-discharge can also occur for RFBs, it is not as significant as that for LIBs, since the majority of the two electrolytes is located in tanks and only a very small volume is located inside the electrochemical cell, which might be affected by chemical diffusion, and thus, cause self-discharge.

High-voltage (> 3 V) batteries still require organic-solvent- or ionic-liquid-based electrolytes (Figure 14). Several promising strategies have been demonstrated to inhibit the dissolution of organic solid-electrode materials, such as the use of concentrated carbonate-based electrolytes, ILs with reduced interaction with organic active materials, or polymer electrolytes with inorganic materials as fillers. Further optimization is needed to obtain better compatibility between the type of organic active materials and selected electrolytes. Moreover, the transition from hybrid lithium (or other metals)/organic material based batteries to all-organic batteries (such as for dual-ion batteries and proton batteries) may enable great flexibility for the selection of suitable electrolytes. In addition, polymer- and ionic-liquid-based electrolytes also allow for the operation of batteries at elevated temperatures, showing largely improved capacities, reaction kinetics, and cycling stability.

For RFBs, nonaqueous electrolytes generally show insufficient power performance, which is related to slow mass transport, sluggish reaction kinetics, and low ionic conductivity of the membrane. Further optimization requires the rational design of the flow channel, cell configuration, use of catalysts, and synthesis/selection of high-performance membranes. Membrane-free RFBs and size-exclusion RFBs with polymer active materials are still at an early stage of research. So far, there is a lack of successful operation of these flow cells at high concentrations and current densities.

## Acknowledgements

R.C. acknowledges financial support from KIST Europe basic research funding, CMBlu Energy AG, and the continuing support from Prof. R. Hempelmann. D.B. and S.P. acknowledge financial support from the Helmholtz Association for basic funding and the German Federal Ministry of Education and Research (BMBF) within the MOLIBE project (03SF0583A). M.S. would like to acknowledge financial support by the BMBF within the Green Talents Initiative. A.B. and P.G. wish to thank the Deutsche Forschungsgemeinschaft (DFG) within the project "Redox-active ionic liquids in redox-flow-batteries" for financial support. S.K. and D.S. appreciate financial support by JLU Giessen with a starting grant within the project VerB. J.C. would like to thank the 111 Project from the Ministry of Education of China (B12015).

## Conflict of interest

The authors declare no conflict of interest.

**Keywords:** electrochemistry • energy storage • ionic liquids • polymers • redox chemistry

- [1] B. Dunn, H. Kamath, J.-M. Tarascon, *Science* **2011**, *334*, 928–935.
- [2] R. Schmich, R. Wagner, G. Hörpel, T. Placke, M. Winter, *Nat. Energy* **2018**, *3*, 267–278.
- [3] M. S. Whittingham, *Chem. Rev.* **2014**, *114*, 11414–11443.
- [4] R. Chen, S. Ren, M. Knapp, D. Wang, R. Witter, M. Fichtner, H. Hahn, *Adv. Energy Mater.* **2015**, *5*, 1401814.
- [5] J. B. Goodenough, K.-S. Park, *J. Am. Chem. Soc.* **2013**, *135*, 1167–1176.
- [6] M. Skyllas-Kazacos, L. Cao, M. Kazacos, N. Kausar, A. Mousa, *ChemSusChem* **2016**, *9*, 1521–1543.
- [7] Y. Liang, Z. Tao, J. Chen, *Adv. Energy Mater.* **2012**, *2*, 742–769.
- [8] Z. Song, H. Zhou, *Energy Environ. Sci.* **2013**, *6*, 2280–2301.
- [9] T. B. Schon, B. T. McAllister, P.-F. Li, D. S. Seferos, *Chem. Soc. Rev.* **2016**, *45*, 6345–6404.
- [10] J. Winsberg, T. Hagemann, T. Janoschka, M. D. Hager, U. S. Schubert, *Angew. Chem. Int. Ed.* **2017**, *56*, 686–711; *Angew. Chem.* **2017**, *129*, 702–729.
- [11] H. Nishide, K. Oyaizu, *Science* **2008**, *319*, 737–738.
- [12] H. Wu, S. A. Shevlin, Q. Meng, W. Guo, Y. Meng, K. Lu, Z. Wei, Z. Guo, *Adv. Mater.* **2014**, *26*, 3338–3343.
- [13] Z. Guo, Y. Ma, X. Dong, J. Huang, Y. Wang, Y. Xia, *Angew. Chem. Int. Ed.* **2018**, *57*, 11737–11741; *Angew. Chem.* **2018**, *130*, 11911–11915.
- [14] Q. Zhao, Y. Lu, J. Chen, *Adv. Energy Mater.* **2017**, *7*, 1601792.
- [15] J. C. Pramudita, D. Sehrawat, D. Goonetilleke, N. Sharma, *Adv. Energy Mater.* **2017**, *7*, 1602911.
- [16] L. Chen, J. L. Bao, X. Dong, D. G. Truhlar, Y. Wang, C. Wang, Y. Xia, *ACS Energy Lett.* **2017**, *2*, 1115–1121.
- [17] Y. Lu, Q. Zhang, L. Li, Z. Niu, J. Chen, *Chem* **2018**, *4*, 2786–2813.
- [18] J. Xie, Q. Zhang, *Small* **2019**, *15*, 1805061.
- [19] X. Wei, W. Pan, W. Duan, A. Hollas, Z. Yang, B. Li, Z. Nie, J. Liu, D. Reed, W. Wang, V. Sprenkle, *ACS Energy Lett.* **2017**, *2*, 2187–2204.
- [20] R. Ye, D. Henkensmeier, S. J. Yoon, Z. Huang, D. K. Kim, Z. Chang, S. Kim, R. Chen, *J. Electrochem. Energy Convers. Storage* **2018**, *15*, 010801.
- [21] Y. Ding, C. Zhang, L. Zhang, Y. Zhou, G. Yu, *Chem. Soc. Rev.* **2018**, *47*, 69–103.
- [22] J. Luo, B. Hu, M. Hu, Y. Zhao, T. L. Liu, *ACS Energy Lett.* **2019**, *4*, 2220–2240.
- [23] P. Leung, A. A. Shah, L. Sanz, C. Flox, J. R. Morante, Q. Xu, M. R. Mohamed, C. Ponce de León, F. C. Walsh, *J. Power Sources* **2017**, *360*, 243–283.
- [24] J. Noack, N. Roznyatovskaya, T. Herr, P. Fischer, *Angew. Chem. Int. Ed.* **2015**, *54*, 9776–9809; *Angew. Chem.* **2015**, *127*, 9912–9947.
- [25] S.-H. Shin, S.-H. Yun, S.-H. Moon, *RSC Adv.* **2013**, *3*, 9095–9116.
- [26] R. Chen, *ChemElectroChem* **2019**, *6*, 603–612.
- [27] J. D. Hofmann, D. Schröder, *Chem. Ing. Tech.* **2019**, *91*, 786–794.
- [28] Y. Liang, Y. Jing, S. Gheyhani, K. Y. Lee, P. Liu, A. Facchetti, Y. Yao, *Nat. Mater.* **2017**, *16*, 841–848.
- [29] X. Dong, Z. Guo, Z. Guo, Y. Wang, Y. Xia, *Joule* **2018**, *2*, 902–913.
- [30] J. Xie, P. Gu, Q. Zhang, *ACS Energy Lett.* **2017**, *2*, 1985–1996.
- [31] J. Kalhoff, G. G. Eshetu, D. Bresser, S. Passerini, *ChemSusChem* **2015**, *8*, 2154–2175.
- [32] Z. Yang, J. Zhang, M. C. W. Kintner-Meyer, X. Lu, D. Choi, J. P. Lemmon, J. Liu, *Chem. Rev.* **2011**, *111*, 3577–3613.
- [33] M. Watanabe, M. L. Thomas, S. Zhang, K. Ueno, T. Yasuda, K. Dokko, *Chem. Rev.* **2017**, *117*, 7190–7239.
- [34] Q. Yang, Z. Zhang, X.-G. Sun, Y.-S. Hu, H. Xing, S. Dai, *Chem. Soc. Rev.* **2018**, *47*, 2020–2064.
- [35] M. H. Chakrabarti, F. S. Mjalli, I. M. AlNashif, M. A. Hashim, M. A. Husain, L. Bahadori, C. T. J. Low, *Renewable Sustainable Energy Rev.* **2014**, *30*, 254–270.
- [36] K. Xu, *Chem. Rev.* **2004**, *104*, 4303–4418.
- [37] B. Häupler, A. Wild, U. S. Schubert, *Adv. Energy Mater.* **2015**, *5*, 1402034.
- [38] P. Peljo, H. H. Girault, *Energy Environ. Sci.* **2018**, *11*, 2306–2309.
- [39] P. Poizat, F. Dolhem, J. Gaubicher, *Curr. Opin. Electrochem.* **2018**, *9*, 70–80.
- [40] P. Poizat, F. Dolhem, *Energy Environ. Sci.* **2011**, *4*, 2003–2019.
- [41] T. Janoschka, M. D. Hager, U. S. Schubert, *Adv. Mater.* **2012**, *24*, 6397–6409.
- [42] S. Muench, A. Wild, C. Friebe, B. Häupler, T. Janoschka, U. S. Schubert, *Chem. Rev.* **2016**, *116*, 9438–9484.
- [43] V. Aravindan, J. Gnanaraj, S. Madhavi, H.-K. Liu, *Chem. Eur. J.* **2011**, *17*, 14326–14346.
- [44] Y. Liang, Y. Yao, *Joule* **2018**, *2*, 1690–1706.
- [45] G. Zubi, R. Dufo-López, M. Carvalho, G. Pasaoglu, *Renewable Sustainable Energy Rev.* **2018**, *89*, 292–308.
- [46] K. Xu, *Chem. Rev.* **2014**, *114*, 11503–11618.
- [47] Y. Liang, Y. Yan, *Gen. Chem.* **2017**, *3*, 207–212.
- [48] M. Armand, F. Endres, D. R. MacFarlane, H. Ohno, B. Scrosati, *Nat. Mater.* **2009**, *8*, 621–629.
- [49] G. B. Appetecchi, M. Montanino, A. Balducci, S. F. Lux, M. Winterb, S. Passerini, *J. Power Sources* **2009**, *192*, 599–605.
- [50] G. A. Elia, J. Hassoun, W.-J. Kwak, Y.-K. Sun, B. Scrosati, F. Mueller, D. Bresser, S. Passerini, P. Oberhumer, N. Tsiouvaras, J. Reiter, *Nano Lett.* **2014**, *14*, 6572–6577.
- [51] D. Bresser, E. Paillard, S. Passerini, *J. Electrochem. Sci. Technol.* **2014**, *5*, 37–44.
- [52] D. R. MacFarlane, M. Forsyth, P. C. Howlett, M. Kar, S. Passerini, J. M. Pringle, H. Ohno, M. Watanabe, F. Yan, W. Zheng, S. Zhang, J. Zhang, *Nat. Rev. Mater.* **2016**, *1*, 15005.
- [53] B. E. Gurkan, Z. Qiang, Y.-M. Chen, Y. Zhu, B. D. Vogt, *J. Electrochem. Soc.* **2017**, *164*, H5093–H5099.
- [54] X. Wang, Z. Shang, A. Yang, Q. Zhang, F. Cheng, D. Jia, J. Chen, *Chem* **2019**, *5*, 364–375.
- [55] C. Karlsson, C. Strietzel, H. Huang, M. Sjödin, P. Jannasch, *ACS Appl. Energy Mater.* **2018**, *1*, 6451–6462.
- [56] J. Qin, Q. Lan, N. Liu, F. Men, X. Wang, Z. Song, H. Zhan, *iScience* **2019**, *15*, 16–27.
- [57] B. E. Conway, V. Birss, J. Wojtowicz, *J. Power Sources* **1997**, *66*, 1–14.
- [58] P. Simon, Y. Gogotsi, B. Dunn, *Science* **2014**, *343*, 1210–1211.
- [59] A. Brandt, S. Pohlmann, A. Varzi, A. Balducci, S. Passerini, *MRS Bull.* **2013**, *38*, 554–559.
- [60] P. Meister, V. Sizios, J. Reiter, S. Klamor, S. Rothermel, O. Fromm, H.-W. Meyer, M. Winter, T. Placke, *Electrochim. Acta* **2014**, *130*, 625–633.
- [61] V. A. Nikitina, R. R. Nazmutdinov, G. A. Tsirlina, *J. Phys. Chem. B* **2011**, *115*, 668–677.
- [62] J.-K. Kim, G. Cheruvally, J.-W. Choi, J.-H. Ahn, D. S. Choi, C. E. Song, *J. Electrochem. Soc.* **2007**, *154*, A839–A843.
- [63] W. Huang, Z. Zhu, L. Wang, S. Wang, H. Li, Z. Tao, J. Shi, L. Guan, J. Chen, *Angew. Chem. Int. Ed.* **2013**, *52*, 9162–9166; *Angew. Chem.* **2013**, *125*, 9332–9336.
- [64] Z. Zhu, M. Hong, D. Guo, J. Shi, Z. Tao, J. Chen, *J. Am. Chem. Soc.* **2014**, *136*, 16461–16464.
- [65] M. Lécuyer, J. Gaubicher, A.-L. Barrès, F. Dolhem, M. Deschamps, D. Guyomard, P. Poizat, *Electrochem. Commun.* **2015**, *55*, 22–25.
- [66] W. Li, L. Chen, Y. Sun, C. Wang, Y. Wang, Y. Xia, *Solid State Ionics* **2017**, *300*, 114–119.
- [67] W. Wei, L. Li, L. Zhang, J. Hong, G. He, *Electrochem. Commun.* **2018**, *90*, 21–25.
- [68] H. Fei, Y. Liu, Y. An, X. Xu, G. Zeng, Y. Tian, L. Ci, B. Xi, S. Xiong, J. Feng, *J. Power Sources* **2018**, *399*, 294–298.
- [69] Q. Zhao, C. Guo, Y. Lu, L. Liu, J. Liang, J. Chen, *Ind. Eng. Chem. Res.* **2016**, *55*, 5795–5804.
- [70] T. Suga, H. Konishi, H. Nishide, *Chem. Commun.* **2007**, 1730–1732.
- [71] S. Lee, G. Kwon, K. Ku, K. Yoon, S.-K. Jung, H.-D. Lim, K. Kang, *Adv. Mater.* **2018**, *30*, 1704682.
- [72] J. Wang, Y. Yamada, K. Sodeyama, C. H. Chiang, Y. Tateyama, A. Yamada, *Nat. Commun.* **2016**, *7*, 12032.
- [73] C. Guo, K. Zhang, Q. Zhao, L. Pei, J. Chen, *Chem. Commun.* **2015**, *51*, 10244–10247.
- [74] L. Suo, Y.-S. Hu, H. Li, M. Armand, L. Chen, *Nat. Commun.* **2013**, *4*, 1481.

- [75] Z. Xu, H. Ye, H. Li, Y. Xu, C. Wang, J. Yin, H. Zhu, *ACS Omega* **2017**, *2*, 1273–1278.
- [76] K. Nakahara, J. Iriyama, S. Iwasa, M. Suguro, M. Satoh, E. J. Cairns, *J. Power Sources* **2007**, *165*, 398–402.
- [77] P. Gerlach, R. Burges, A. Lex-Balducci, U. S. Schubert, A. Balducci, *Electrochim. Acta* **2019**, *306*, 610–616.
- [78] P. Gerlach, R. Burges, A. Lex-Balducci, U. S. Schubert, A. Balducci, *J. Power Sources* **2018**, *405*, 142–149.
- [79] D. Bin, Y. Wen, Y. Wang, Y. Xia, *J. Energy Chem.* **2018**, *27*, 1521–1535.
- [80] J. Huang, Z. Guo, Y. Ma, D. Bin, Y. Wang, Y. Xia, *Small Methods* **2019**, *3*, 1800272.
- [81] J.-Y. Luo, W.-J. Cui, P. He, Y.-Y. Xia, *Nat. Chem.* **2010**, *2*, 760–765.
- [82] Z. Chang, Y. Yang, M. Li, X. Wang, Y. Wu, *J. Mater. Chem. A* **2014**, *2*, 10739–10755.
- [83] W. Li, J. R. Dahn, D. S. Wainwright, *Science* **1994**, *264*, 1115–1118.
- [84] W. Tang, Y. Zhu, Y. Hou, L. Liu, Y. Wu, K. P. Loh, H. Zhang, K. Zhu, *Energy Environ. Sci.* **2013**, *6*, 2093–2104.
- [85] D. J. Kim, Y. H. Jung, K. K. Bharathi, S. H. Je, D. K. Kim, A. Coskun, J. W. Choi, *Adv. Energy Mater.* **2014**, *4*, 1400133.
- [86] X. Dong, H. Yu, Y. Ma, J. L. Bao, D. G. Truhlar, Y. Wang, Y. Xia, *Chem. Eur. J.* **2017**, *23*, 2560–2565.
- [87] L. Suo, O. Borodin, T. Gao, M. Olguin, J. Ho, X. L. Fan, C. Luo, C. S. Wang, K. Xu, *Science* **2015**, *350*, 938–943.
- [88] L. Suo, O. Borodin, W. Sun, X. Fan, C. Yang, F. Wang, T. Gao, Z. Ma, M. Schroeder, A. Von Cresce, S. M. Russell, M. Armand, A. Angell, K. Xu, C. Wang, *Angew. Chem. Int. Ed.* **2016**, *55*, 7136–7141; *Angew. Chem.* **2016**, *128*, 7252–7257.
- [89] Y. Yamada, K. Usui, K. Sodeyama, S. Ko, Y. Tateyama, A. Yamada, *Nat. Energy* **2016**, *1*, 16129.
- [90] C. Yang, J. Chen, T. Qing, X. Fan, W. Sun, A. von Cresce, M. S. Ding, O. Borodin, J. Vatamanu, M. A. Schroeder, N. Eidson, C. Wang, K. Xu, *Joule* **2017**, *1*, 122–132.
- [91] Q. Zhao, W. Huang, Z. Luo, L. Liu, Y. Lu, Y. Li, L. Li, J. Hu, H. Ma, J. Chen, *Sci. Adv.* **2018**, *4*, eaao1761.
- [92] Y. Matsuda, K. Tanaka, M. Okada, Y. Takasu, M. Morita, T. Matsumura-Inoue, *J. Appl. Electrochem.* **1988**, *18*, 909–914.
- [93] Z. Li, S. Li, S. Liu, K. Huang, D. Fang, F. Wang, S. Peng, *Electrochem. Solid-State Lett.* **2011**, *14*, A171–A173.
- [94] W. Wang, W. Xu, L. Cosimbescu, D. Choi, L. Li, Z. Yang, *Chem. Commun.* **2012**, *48*, 6669–6671.
- [95] C. S. Sevov, R. E. M. Broner, E. Chénard, R. S. Assary, J. S. Moore, J. Rodríguez-López, M. S. Sanford, *J. Am. Chem. Soc.* **2015**, *137*, 14465–14472.
- [96] X. Wei, W. Xu, J. Huang, L. Zhang, E. Walter, C. Lawrence, M. Vijayakumar, W. A. Henderson, T. Liu, L. Cosimbescu, B. Li, V. Sprenkle, W. Wang, *Angew. Chem. Int. Ed.* **2015**, *54*, 8684–8687; *Angew. Chem.* **2015**, *127*, 8808–8811.
- [97] K. Gong, Q. Fang, S. Gu, S. F. Y. Li, Y. Yan, *Energy Environ. Sci.* **2015**, *8*, 3515–3530.
- [98] L. Su, M. Ferrandon, J. L. Barton, N. U. de la Rosa, J. T. Vaughey, F. R. Brushett, *Electrochim. Acta* **2017**, *246*, 251–258.
- [99] M. Taggougui, B. Carré, P. Willmann, D. Lemordant, *J. Power Sources* **2007**, *174*, 643–647.
- [100] Z. Zhang, L. Zhang, J. A. Schlueter, P. C. Redfern, L. Curtiss, K. Amine, *J. Power Sources* **2010**, *195*, 4957–4962.
- [101] J. Huang, L. Cheng, R. S. Assary, P. Wang, Z. Xue, A. K. Burrell, L. A. Curtiss, L. Zhang, *Adv. Energy Mater.* **2015**, *5*, 1401782.
- [102] K. Takechi, Y. Kato, Y. Hase, *Adv. Mater.* **2015**, *27*, 2501–2506.
- [103] W. Wang, Q. Luo, B. Li, X. Wei, L. Li, Z. Yang, *Adv. Funct. Mater.* **2013**, *23*, 970–986.
- [104] S. Schaltin, Y. Li, N. R. Brooks, J. Snickers, I. F. J. Vankelecom, K. Binne-mans, J. Fransaer, *Chem. Commun.* **2016**, *52*, 414–417.
- [105] C. A. Appleby, D. M. Stewart, R. T. Fryer, J. C. Sell, H. D. Pratt, III, T. M. Anderson, R. W. Meulenber, *Electrochim. Acta* **2015**, *185*, 156–161.
- [106] K. Periyapperuma, Y. Zhang, D. R. MacFarlane, M. Forsyth, C. Pozo-Gonzalo, P. C. Howlett, *ChemElectroChem* **2017**, *4*, 1051–1058.
- [107] Y. H. Wen, H. M. Zhang, P. Qian, H. T. Zhou, P. Zhao, B. L. Yi, Y. S. Yang, *Electrochim. Acta* **2006**, *51*, 3769–3775.
- [108] D. Zhang, Q. Liu, X. Shi, Y. Li, *J. Power Sources* **2012**, *203*, 201–205.
- [109] G. P. Rajarathnam, M. E. Easton, M. Schneider, A. F. Masters, T. Maschmeyer, A. M. Vassallo, *RSC Adv.* **2016**, *6*, 27788–27797.
- [110] R. Chen, D. Henkensmeier, S. Kim, S. J. Yoon, T. Zinkevich, S. Indris, *ACS Appl. Energy Mater.* **2018**, *1*, 6047–6055.
- [111] M. Zhou, Q. Huang, T. N. P. Truong, J. Ghilane, Y. G. Zhu, C. Jia, R. Yan, L. Fan, H. Randriamahazaka, Q. Wang, *Chem* **2017**, *3*, 1036–1049.
- [112] G. Hernández, M. İşik, D. Mantione, A. Pendashteh, P. Navalpotro, D. Shanmukaraj, R. Marcilla, D. Mecerreyes, *J. Mater. Chem. A* **2017**, *5*, 16231–16240.
- [113] Y. Zhang, R. Ye, D. Henkensmeier, R. Hempelmann, R. Chen, *Electrochim. Acta* **2018**, *263*, 47–52.
- [114] M. A. Bhat, *Electrochim. Acta* **2012**, *81*, 275–282.
- [115] P. Navalpotro, J. Palma, M. Anderson, R. Marcilla, *J. Power Sources* **2016**, *306*, 711–717.
- [116] X. Wang, X. Xing, Y. Huo, Y. Zhao, Y. Li, H. Chen, *Int. J. Electrochem. Sci.* **2018**, *13*, 6676–6683.
- [117] I. A. Popov, B. L. Davis, R. Mukundan, E. R. Batista, P. Yang, *Front. Phys.* **2019**, *6*, 141.
- [118] A. Ejigu, P. A. Greatorex-Davies, D. A. Walsh, *Electrochem. Commun.* **2015**, *54*, 55–59.
- [119] T. Tamura, K. Yoshida, T. Hachida, M. Tsuchiya, M. Nakamura, Y. Kazue, N. Tachikawa, K. Dokko, M. Watanabe, *Chem. Lett.* **2010**, *39*, 753–755.
- [120] R. Chen, R. Hempelmann, *Electrochem. Commun.* **2016**, *70*, 56–59.
- [121] P. Huang, P. Zhang, X. Gao, D. Henkensmeier, S. Passerini, R. Chen, *ACS Appl. Energy Mater.* **2019**, *2*, 3773–3779.
- [122] R. Chen, R. Ye, R. Hempelmann, S. Kim, A. Möller, J. Hartwig, N. Krawczyk, P. Geigle, *WO2019174910*, **2019**.
- [123] Z. Huang, C. W. M. Kay, B. Kuttich, D. Rauber, T. Kraus, H. Li, S. Kim, R. Chen, *Nano Energy* **2020**, *69*, 104464.
- [124] P. Navalpotro, J. Palma, M. Anderson, R. Marcilla, *Angew. Chem. Int. Ed.* **2017**, *56*, 12460–12465; *Angew. Chem.* **2017**, *129*, 12634–12639.
- [125] Z. Yuan, H. Zhang, X. Li, *Chem. Commun.* **2018**, *54*, 7570–7588.
- [126] J. Winsberg, S. Benndorf, A. Wild, M. D. Hager, U. S. Schubert, *Macromol. Chem. Phys.* **2018**, *219*, 1700267.
- [127] E. C. Montoto, Y. Cao, K. Hernández-Burgos, C. S. Sevov, M. N. Braten, B. A. Helms, J. S. Moore, J. Rodríguez-López, *Macromolecules* **2018**, *51*, 3539–3546.
- [128] G. Nagarjuna, J. Hui, K. J. Cheng, T. Lichtenstein, M. Shen, J. S. Moore, J. Rodríguez-López, *J. Am. Chem. Soc.* **2014**, *136*, 16309–16316.
- [129] E. Zanzola, C. R. Dennison, A. Battistel, P. Peljo, H. Vrubel, V. Amstutz, H. H. Girault, *Electrochim. Acta* **2017**, *235*, 664–671.
- [130] A. Mukhopadhyay, J. Hamel, R. Katahira, H. Zhu, *ACS Sustainable Chem. Eng.* **2018**, *6*, 5394–5400.
- [131] M. Burgess, J. S. Moore, J. Rodríguez-López, *Acc. Chem. Res.* **2016**, *49*, 2649–2657.
- [132] E. C. Montoto, N. Gavvalapalli, J. Hui, M. Burgess, N. M. Sekerak, K. Hernández-Burgos, T. Wei, M. Kneer, J. Grolman, K. J. Cheng, *J. Am. Chem. Soc.* **2016**, *138*, 13230–13237.
- [133] K. H. Hendriks, S. G. Robinson, M. N. Braten, C. S. Sevov, B. A. Helms, M. S. Sigman, S. D. Minter, M. S. Sanford, *ACS Cent. Sci.* **2018**, *4*, 189–196.
- [134] S. H. Oh, C. W. Lee, D. H. Chun, J. D. Jeon, J. Shim, K. H. Shin, J. H. Yang, *J. Mater. Chem. A* **2014**, *2*, 19994–19998.
- [135] S. E. Doris, A. L. Ward, A. Baskin, P. D. Frischmann, N. Gavvalapalli, E. Chénard, C. S. Sevov, D. Prendergast, J. S. Moore, B. A. Helms, *Angew. Chem. Int. Ed.* **2017**, *56*, 1595–1599; *Angew. Chem.* **2017**, *129*, 1617–1621.
- [136] M. J. Baran, M. N. Braten, S. Sahu, A. Baskin, S. M. Meckler, L. Li, L. Maserati, M. E. Carrington, Y. M. Chiang, D. Prendergast, B. A. Helms, *Joule* **2019**, *3*, 2968–2985.
- [137] Z. T. Gossage, N. B. Schorr, K. Hernández-Burgos, J. Hui, B. H. Simpson, E. C. Montoto, J. Rodríguez-López, *Langmuir* **2017**, *33*, 9455–9463.
- [138] W. Yan, C. Wang, J. Tian, G. Zhu, L. Ma, Y. Wang, R. Chen, Y. Hu, L. Wang, T. Chen, J. Ma, Z. Jin, *Nat. Commun.* **2019**, *10*, 2513.
- [139] T. Janoschka, S. Morgenstern, H. Hiller, C. Friebe, K. Wolkersdörfer, B. Häupler, M. D. Hager, U. S. Schubert, *Polym. Chem.* **2015**, *6*, 7801–7811.
- [140] J. Winsberg, T. Hagemann, S. Muench, C. Friebe, B. Häupler, T. Janoschka, S. Morgenstern, M. D. Hager, U. S. Schubert, *Chem. Mater.* **2016**, *28*, 3401–3405.
- [141] Y. Xu, Y. Wen, J. Cheng, G. Cao, Y. Yang, *Electrochem. Commun.* **2009**, *11*, 1422–1424.



- [142] B. Huskinson, M. P. Marshak, C. Suh, S. Er, M. R. Gerhardt, C. J. Galvin, X. Chen, A. Aspuru-Guzik, R. G. Gordon, M. J. Aziz, *Nature* **2014**, *505*, 195–198.
- [143] B. Li, J. Liu, *Natl. Sci. Rev.* **2017**, *4*, 91–105.
- [144] B. Yang, L. Hooper-Burkhardt, F. Wang, G. K. Surya Prakash, S. R. Narayanan, *J. Electrochem. Soc.* **2014**, *161*, A1371–A1380.
- [145] R. van Noorden, *Nature* **2014**, *507*, 26–28.
- [146] J. D. Hofmann, F. L. Pfanschilling, N. Krawczyk, P. Geigle, L. Hong, S. Schmalisch, H. A. Wegner, D. Mollenhauer, J. Janek, D. Schröder, *Chem. Mater.* **2018**, *30*, 762–774.
- [147] K. Lin, Q. Chen, M. R. Gerhardt, L. Tong, S. B. Kim, L. Eisenach, A. W. Valle, D. Hardee, R. G. Gordon, M. J. Aziz, M. P. Marshak, *Science* **2015**, *349*, 1529–1532.
- [148] Z. Yang, L. Tong, D. P. Tabor, E. S. Beh, M.-A. Goulet, D. de Porcellinis, A. Aspuru-Guzik, R. G. Gordon, M. J. Aziz, *Adv. Energy Mater.* **2018**, *8*, 1702056.
- [149] K. Lin, R. Gómez-Bombarelli, E. S. Beh, L. Tong, Q. Chen, A. Valle, A. Aspuru-Guzik, M. J. Aziz, R. G. Gordon, *Nat. Energy* **2016**, *1*, 16102.
- [150] C. Zhang, Z. Niu, S. Peng, Y. Ding, L. Zhang, X. Guo, Y. Zhao, G. Yu, *Adv. Mater.* **2019**, *31*, 1901052.
- [151] Z. Chang, D. Henkensmeier, R. Chen, *J. Power Sources* **2019**, *418*, 11–16.
- [152] K. Wedege, E. Dražević, D. Konya, A. Bentien, *Sci. Rep.* **2016**, *6*, 39101.
- [153] H. Alt, H. Binder, G. Klempert, A. Köhling, G. Sandstedt, *J. Appl. Electrochem.* **1972**, *2*, 193–200.
- [154] Y. Ji, M.-A. Goulet, D. A. Pollack, D. G. Kwabi, S. Jin, D. Porcellinis, E. F. Kerr, R. G. Gordon, M. J. Aziz, *Adv. Energy Mater.* **2019**, *9*, 1900039.
- [155] S. Jin, Y. Jing, D. G. Kwabi, Y. Ji, L. Tong, D. de Porcellinis, M.-A. Goulet, D. A. Pollack, R. G. Gordon, M. J. Aziz, *ACS Energy Lett.* **2019**, *4*, 1342–1348.
- [156] S. Er, C. Suh, M. P. Marshak, A. Aspuru-Guzik, *Chem. Sci.* **2015**, *6*, 885–893.
- [157] M. R. Gerhardt, L. Tong, R. Gómez-Bombarelli, Q. Chen, M. P. Marshak, C. J. Galvin, A. Aspuru-Guzik, R. G. Gordon, M. J. Aziz, *Adv. Energy Mater.* **2017**, *7*, 1601488.
- [158] B. Hu, C. DeBruler, Z. Rhodes, T. L. Liu, *J. Am. Chem. Soc.* **2017**, *139*, 1207–1214.
- [159] M. Gauthier, T. J. Carney, A. Grimaud, L. Giordano, N. Pour, H.-H. Chang, D. P. Fenning, S. F. Lux, O. Paschos, C. Bauer, F. Maglia, S. Lupart, P. Lamp, Y. Shao-Horn, *J. Phys. Chem. Lett.* **2015**, *6*, 4653–4672.
- [160] M. Hayyan, F. S. Mjalli, M. A. Hashim, I. M. AlNashef, T. X. Mei, *J. Ind. Eng. Chem.* **2013**, *19*, 106–112.
- [161] R. Chen, *Curr. Opin. Electrochem.* **2020**, *21*, 40–45.

---

Manuscript received: December 10, 2019

Revised manuscript received: January 29, 2020

Accepted manuscript online: January 29, 2020

Version of record online: March 20, 2020